TECHNISCHE UNIVERSITÄT WIEN
Vienna | Austria

Master Thesis

Deposition of polymer-derived ceramic layers with asymmetric porosity

Technische Universität Wien
Institute of Chemical Technologies and Analytics
Getreidemarkt 9/164-CT
1060 Wien

Under supervision of Assistant Prof. Dr. Thomas Konegger
and Ao. Univ. Prof. Dipl.-Ing. Dr.techn. Roland Haubner

Johannes Rauchenecker
Enenkelstraße 18/10
1160 Wien

Vienna, 12.06.2018

Acknowledgements

I would like to thank my supervisors, Roland Haubner and Thomas Konegger for enabling me to work on my master thesis in the project group “High performance ceramics”. They were always available if I had questions or needed input on solutions to problems I encountered during my work.
I am also very grateful for the funding of the project through the Austrian science fund FWF (P-29058-N34).
Furthermore, I want to thank all colleagues from the project group, first and foremost Christina Drechsel, who always offered valuable comments on challenges I had to face.
I also express my gratitude to Gernot Peer from the research group for “Polymer Chemistry and Technology” for measuring the rheological properties of the aqueous slurries I prepared.
A special thanks goes out to my colleagues from the second floor and the members of our bouldering group who helped me to get things off my mind, if experiments did not go according to plan.
Lastly I want to thank all my friends, family and especially my partner Helene who supported and encouraged me during my studies at the TU Wien.

Abstract

Deposition of porous polymer derived ceramic layers onto tubular macroporous silicon nitride substrates via dip coating was investigated. The aim was to establish a process that would allow the preparation of polymer-derived ceramic multilayer membranes with respect to their gas separation properties.

As a first step, silicon nitride supports were prepared following a previously developed procedure. Properties of the newly produced samples were compared to previous results.

Before developing a coating method for the substrates a masking procedure was developed. Two different methods - immersion and dip coating - to apply a polystyrene masking layer from highly concentrated PS solutions in toluene were investigated.

After establishing a masking procedure, the substrates were dip coated with an intermediate layer and/or a top layer.

One layer was applied with an organic slurry of poly(vinyl)silazane and silicon nitride powder in n-hexane, and, after pyrolysis, was supposed to fulfill the role of an intermediate layer, bridging a microporous separation layer and the macroporous substrate.

The second layer was applied by dip coating with a solution of poly(vinyl)silazane in n-hexane. After pyrolysis, this should resemble an actual microporous separation layer of a ceramic membrane. The samples were either directly coated with this layer or first with an intermediate layer followed by this layer.

The samples were characterized by secondary electron microscopy to determine properties like layer thickness and layer adhesion on the substrates, as well as defects in the surface or infiltration behavior of the deposition liquids.

A method to mask the macroporous substrates was developed. Even though infiltration of the deposition liquids was still present in most of the samples, it could be reduced. The masking allowed for the deposition of an intermediate layer without it exhibiting a slip casting-like behavior, which in turn would lead to delamination of the layer.

It was found, that layer quality depends largely on the surface and masking quality of the substrates. Intermediate layers that were deposited did not allow for a more homogenous and defect-free deposition of the separation layer, even though their surfaces were much smoother than the substrate surfaces. Direct application of separation layers led to the most promising results in terms of layer homogeneity and reproducibility.

Kurzfassung

Die Beschichtung von tubularen makroporösen Siliziumnitridsubstraten mit polymerabgeleiteten keramischen Schichten mittels Tauchbeschichtung sollte untersucht werden. Das Ziel war die Entwicklung einer Methode, die es erlaubt, keramische Mehrschichtmembranen herzustellen, um diese in weiterer Folge auf ihre Gastrennungseigenschaften untersuchen können.

In einem ersten Schritt wurden die Siliziumnitridsubstrate über Schlickerguss in einem bereits etablierten Prozess hergestellt. Die Eigenschaften wie Permeabilität und Porosität der hergestellten Substrate wurden mit den bereits von früheren Arbeiten bekannten Eigenschaften verglichen.

Bevor die tubularen Substrate beschichtet werden konnten, musste ein Weg gefunden werden, die Makroporen des Substrats zu maskieren. Zwei unterschiedliche Methoden, Immersion und Tauchbeschichtung, um die Maskierung mit einer hochkonzentrierten Polystyrol-Lösung in Toluol aufzutragen, wurden untersucht.

Nachdem eine funktionierende Maskierungsmethode gefunden worden war, wurden auf die Substrate zwei unterschiedliche Schichten aufgebracht.

Die erste Schicht, eine Intermediärschicht, wurde über Tauchbeschichtung in einen organischen Schlicker aus Siliciumnitridpulver, Poly(vinyl)silazan und n-Hexan aufgebracht. Diese Schicht sollte eine Brückenfunktion zwischen einer mikroporösen Membranschicht und dem makroporösen Substrat übernehmen.

Die zweite Schicht, eine mikroporöse Membranschicht, wurde ebenfalls über Tauchbeschichtung, diesmal allerdings in eine Lösung aus Poly(vinyl)silazan und n-Hexan ohne Siliciumnitridpulver, auf die bereits mit einer Zwischenschicht versehenen Substrate aufgebracht. Maskierte Substrate wurden zum Teil auch direkt mit der mikroporösen Schicht beschichtet, um zu untersuchen, ob eine Zwischenschicht notwendig ist.

Die Proben wurden über Rasterelektronenmikroskopie untersucht. Vor allem die Dicke der Schichten, eventuelle Oberflächendefekte und Infiltrationsverhalten waren von Interesse.

Eine Methode um die tubularen Substrate zu maskieren wurde entwickelt. Trotz dieser Maskierung kommt es allerdings zur Infiltration der Substrate. Nichtsdestotrotz, ermöglicht die Maskierung die Aufbringung von intermediären Schichten, ohne dass dabei schlickergussähnliches Verhalten, welches in Folge zur Delamination der aufgebrachten Schicht führen würde, beobachtet werden konnte.

Weiters wurde beobachtet, dass die Beschichtungsqualität stark von der Oberflächenqualität der Substrate, sowie der Maskierung abhängt. Intermediäre Schichten, welche eine gleichmäßigere Oberfläche als die Substrate zeigten, führten nicht zu fehlerfreien Separationsschichten. Die direkte Beschichtung der maskierten Substrate mit der Trennschicht führte zu den vielversprechendsten Ergebnissen im Hinblick auf Homogenität und Defektfreiheit.

Table of contents

1 Introduction and motivation

Many of today's processes require a way to efficiently separate hydrogen from other gases. An example is the steam reforming process of hydrocarbons which produces a gas mixture mainly consisting of CO, CO_2 and H_2. In this process the following reaction (shown for methane) takes place [1].

$$CH_4 + H_2O \rightarrow CO + 3\,H_2$$

The efficiency of the reaction and the purity of the acquired hydrogen is largely dependent on the ability to separate the reaction gases. Nowadays separation is often times accomplished by absorption or adsorption processes. However, the processes are expensive, which is adequate if hydrogen is seen as a high quality material, but not if it is seen as an alternative to current fuels. By using membrane reactors, the temperature needed for reforming and purification could be lowered, leading to a more energy efficient process. However, membrane technologies that are readily available today, such as polymeric membranes, cannot withstand the high temperatures of the gases [2].

This is where ceramic membranes come into play. Ceramic membranes show a host of advantages, like thermal and chemical stability. However, not all of them may be chemically compatible for said processes; additionally, synthesis of defect-free membranes may prove to be challenging. For example, amorphous silica membranes provide high selectivity for H_2 but are not hydrothermally stable, which renders them unusable for steam reforming. Zeolite membranes on the other hand would be stable, but are difficult to produce without defects, which would eventually lower H_2 selectivity [2, 3].

In recent years the possibility of using polymer derived ceramics (PDCs) for membrane purposes has been researched and a few candidates look very promising. Many research groups have investigated ceramic polymer derived membranes (see Table 1). However, most of the research has been done on different systems and only one research group (Mori et al. [4]) has used a polysilazane to obtain SiCN membrane layers on silicon nitride substrates. What sets their research apart from the research done in this work is that we introduce the masking of the substrates into the production process. This is thought to prevent infiltration of the substrates with the deposition liquids.

Based on this, the following points were set as goals for the thesis:

- Developing a procedure to obtain homogenous and defect-free ceramic coatings on porous tubular silicon nitride substrates with high reproducibility, with the limitation that the coatings should only consist of poly(vinyl)silazane derived material or a combination of the PDC (polymer derived ceramic) with silicon nitride powder for the intermediate layer.
- Establishing a method to mask the macropores of the substrate in order to prevent infiltration of the deposition fluids.
- Testing of different modifications of the deposition method.
- Investigation of the necessity whether an intermediate layer between the macroporous substrate and the separation layer is required.

2 Theoretical background

2.1 Silicon nitride

Silicon nitride is a non-oxidic ceramic which is mostly used in applications where high stability in hot and corrosive environments is required. However, a melting temperature of silicon nitride cannot be defined, since it decomposes at 1877 °C [5]. Typical properties are shown below [6]. The values refer to sintered silicon nitride. It also has to be noted that its properties are highly dependent on the type and amount of sintering additives and sintering method used.

- Density: 3.2 to 3.6 g/cm³
- Coefficient of thermal expansion: 2.9 to 3.9 10^{-6}/K (from 25 to 1000 °C)
- Thermal conductivity: 30.1 W/(m·K) at room temperature
- Young's modulus: 195 GPa at 20 °C
- Flexural strength: 275 to 840 MPa
- Electrical resistivity: >10^{13} (Ohm·cm)

Three different crystal structures of silicon nitride are known. Cubic γ-Si_3N_4 is metastable at standard conditions but it can only be synthesized under a pressure of 15 to 30 GPa at a temperature of 2800 K. α-Si_3N_4 is most commonly obtained when producing silicon nitride powders. It crystallizes in a trigonal structure. During sintering it is converted to the hexagonal β-Si_3N_4 which then shows rod-like crystal growth. If β-rich powder is used, then instead of a rod-like structure it shows globular growth during sintering. Since silicon nitride readily decomposes at temperatures above 1850 °C, sintering additives have to be used in order to lower sintering temperatures. Sintering additives include Oxides like Al_2O_3 or Y_2O_3 which form eutectic melts with surface oxides on the silicon nitride powder. The nitride then dissolves in this melt and crystals grow due to precipitation on existing grains [5].
The properties mentioned above make silicon nitride an appropriate material for cutting applications, roller bearings, sealing rings, as well as high temperature applications like small rocket thrusters [7, 8].

2.2 Polymer derived ceramics

The traditional way of producing ceramics is by forming green bodies from ceramic powders with different techniques, and then sintering them at high temperatures, which leads to consolidation of the particles.
Another way to produce ceramics is by pyrolysis of preceramic polymers, which are most often silicon based. The most distinct advantage of this production route lies in the superior shaping possibilities for polymers compared to ceramics.
Different types of ceramics can be obtained by using different types of preceramic polymers. Figure 1 shows examples for polymers and which ceramics can be produced using them as precursors.

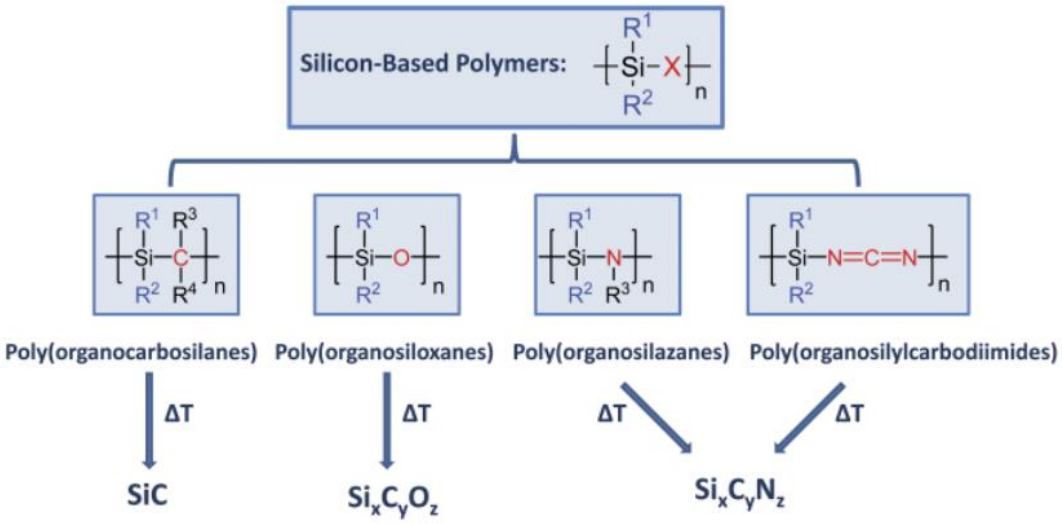

Figure 1: Schematic of pyrolysis products of different preceramic polymers [9]. Reprinted with permission of John Wiley and Sons.

The general production route is as follows: the precursors generally come in the form of oligomers or polymers which can be liquid or solid. These precursors can be shaped via a large variety of processes usually employed in polymer engineering. After shaping, the precursors are crosslinked to form a stable network. Examples for crosslinking would be by radical reactions or condensation reactions.

By using catalysts or initiators, the reactions may be carried out at lower temperatures or even non-thermally, e.g.by using UV-active initiators.

The crosslinked body is then pyrolyzed (decomposed in inert or reactive atmosphere) to obtain a ceramic. By controlling the pyrolysis parameters, the formation of its microstructure can be influenced [10, 11].

2.3 Porous ceramics as membrane materials

Porous materials may be classified by their pore sizes which leads to three main groups. Macroporous materials feature pores with diameters larger than 50 nm, mesopores range from 2 to 50 nm and micropores are pores with less than 2 nm diameter [12]. Chapter 2.3.1 gives an overview of production processes of macroporous materials. However, for many membrane processes, micropores are needed. One way to obtain microporous polymer-derived ceramic materials is through controlling the pyrolysis parameters in the preceramic polymer to ceramic conversion. The resulting microstructure is dependent on the type and structure of polymer used, as well as the heating rate and holding temperature during pyrolysis [10, 11, 13].

One prospective field of application for porous ceramic membranes is gas separation at high temperatures. There are three main requirements for gas membranes: they should exhibit high selectivity for the desired product gas, while also allowing high flow rates and sufficient mechanical stability to withstand pressure differences.

The separation is achieved by gas-selective diffusion through micropores (mostly below 1 nm) in the ceramic material. To counteract the slow diffusion through the micropores the separation layer should be kept as thin as possible to allow for high flow rates. However, the thin layer by itself cannot withstand the pressure differences necessary for operation, which is why the separation layer is often applied onto the surface of a macroporous (pore size > 50 nm) substrate. A mesoporous intermediate layer usually acts as a bridging layer, connecting the substrate and the separation layer [14].

A possible solution to obtain membranes that offer good selectivity, permeability and mechanical properties is to produce asymmetric membranes that are built from multiple layers, each of which takes on different tasks [14].

The macroporous support layer acts as a substrate onto which other components can be coated and which provides the necessary mechanical properties. Its macropores offer high permeability and basically no selectivity. An intermediate layer may be coated onto the support, which has smaller pores, usually in the mesopore range (2 to 50 nm), but is also much thinner and so the decrease in permeability can be kept in check. It acts as a bridge between the support and the separation layer and offers a smooth surface that is better suited for applying a microporous layer. The separation layer for gas separation purposes is microporous; it should show good selectivity for the desired product gas, but it also hinders the flow of all gases, which is why it must be kept thin. In any case the separation layer often times cannot be coated directly onto the macroporous support, since it can infiltrate the pores [14].

Table 1 shows an overview of different ceramic membranes produced using preceramic polymers. Shown in the table are the support materials used, whether or not an intermediate layer was deposited, and what material the separation layer/s was/were composed of (with the preceramic polymer type used in brackets). Further columns show the number of deposition steps for the separation layer, whether or not a masking was used, and the geometry of the samples.

Table 1: Overview of different ceramic membranes with polymer derived membrane layers.

Support material	Intermediate layer material	Separation layer material	Number of separation layer coatings	Masking	Geometry	Reference
α-Al_2O_3	γ-Al_2O_3 + ZrO_2	SiOC (Polysiloxane)	?	no	tubular	[15]
α-Al_2O_3	γ-Al_2O_3 + ZrO_2	SiCN (Polysilazane, PSZ)	?	no	tubular	[15]
α-Al_2O_3	γ-Al_2O_3	SiBCN	3	no	tubular	[16]
α-Al_2O_3	γ-Al_2O_3	SiC PCS	1	no	tubular	[17]
α-Al_2O_3	γ-Al_2O_3	SiC (PCS/PVS) (radiation cured)	?	no	disc	[3]
α-Al_2O_3	-	SiC (PCS)	4	no	tubular	[18]
SiC	SiC	SiOC (PDMS)	1	no	tubular	[19]
SiC	fibers from AHPCS	SiC (AHPCS)	up to 6	PS sacrificial interlayer	tubular	[20]
Si_3N_4	Si_3N_4+ PSZ	SiCN (PSZ)	up to 2	no	tubular	[4]
Si_3N_4	Yes*	Si-N (PSZ)	?	?	tubular	[21]
Si_3N_4	PSZ	Silica (PSZ-derived)	4 (IL) 3 (TL)	no	disc	[22]

**no further information could be gathered, since the publication refers to a Japanese patent which could not be accessed.*

2.3.1 Fabrication processes of macroporous ceramics

Many processes are known for the production of macroporous ceramics. Five simple examples have been picked to be described.

Partial Sintering

In partial sintering a green body made from powder is sintered but before reaching full density the process is interrupted. Parameters that influence the porosity of the sintered ceramic part are:

- Forming pressure and green density
- Additives
- Sintering temperature and holding time

As a rule of thumb the pore diameters can be estimated to be roughly one fifth to half of the particle diameter. By partial sintering porosities of up to 50 % can be reached [23].

Sacrificial Fugitives

Another way to introduce porosity into ceramics is by using sacrificial fillers as pore forming agents. This is done by mixing sacrificial fugitives of a specified size with the ceramic powder or a preceramic polymer. The sacrificial fugitives are solids that can be removed (e.g. by burning out) before sintering or pyrolysis of the polymer, leaving behind pores that show the inverted geometry of the fillers. A problem of this route, however, is that the gases need ways to escape the solid, which can lead to cracks if the burnout procedure chosen was too aggressive. Examples for sacrificial fillers are polyethylene beads [24], PMMA [25], or starch [26].

Freeze Casting

Freeze casting is a variant of the sacrificial fugitive approach. A stable dispersion of ceramic particles and binder in a solvent is frozen with a controlled cooling rate. Upon solidification the powder particles are driven out of the dispersion and concentrated between the solid solvent crystals which often grow in a lamellar structure. The solvent is then sublimated (for example by using a freeze dryer) and the green body is sintered. The sintered part represents a negative of the initially frozen solvent crystals. Water or camphene are often used as solvents [27].

Replica Templates

Porosity can also be obtained by replicating an organic template with ceramics. It is done by submerging the template (polymeric foam, wood,…) in a ceramic slurry and then removing excess slurry from the template pores by either squeezing or centrifuging it. The template is then burned out before sintering the ceramic.
A lot of possible template materials are synthetic, like polymeric foams. However, there are also works that describe using natural templates like wood or corals as templates [28].

One problem of this technique is that the struts of the ceramic are hollow, which leads to reduced mechanical properties, however, there are ways to counteract this [29].

Direct foaming

In direct foaming a ceramic foam is produced by introducing gas into a ceramic slurry or preceramic polymer [30].

There are two ways to disperse a gas in a liquid. The gas could either be blown into the liquid from an external source or it could be generated in situ, by utilizing chemical reactions (e.g. thermal decomposition reactions) that yield gaseous products.

By using surfactants, a foam can be generated and stabilized. If a preceramic polymer is used, the foam has to be stabilized until crosslinking has taken place and the polymer is solid. If a ceramic slurry is used there are usually gelating agents included or also organic monomers which polymerize after foaming. They stabilize the foam upon solidification and get burned out before sintering [31, 32].

Table 2 shows some fabrication processes for macroporous ceramics.

Table 2: Overview of obtainable pore sizes with different fabrication processes for macroporous ceramics according to [23].

	Minimum pore size	Maximum pore size
Partial sintering	50 nm	20 mm
Sacrificial Fugitives	50 nm	> 100 mm
Replica Templates	1 mm	> 100 mm
Direct Foaming	3 mm	> 100 mm

2.4 Thin-film deposition onto porous substrates from liquid phase by dip-coating

Over the course of years many techniques to apply thin solid films as coatings onto support materials have been developed. Thin film deposition techniques can be divided into two major groups: dry and liquid techniques. Dry techniques, such as Chemical or Physical Vapor Deposition will not be discussed in this work.

A lot of factors have to be taken into consideration when choosing a deposition technique. It is often the case that more simplistic methods are used, as they are easier to establish in newly developed (or still developing) processes.

One of the simplest techniques to implement is dip-coating, which will be the focus of the following chapters.

2.4.1 Deposition by dip coating

Dip coating as a method for the deposition of thin films has a lot of advantages over other application methods. Its biggest advantages over other processing methods lie in its simplicity and low cost.

The substrate is dipped into a solution containing precursors for the coating (e.g. in sol-gel processes) or a dispersion containing particles that will make up the final coating. After a set amount of time the substrate is removed from the dip coating liquid at a controlled rate. During removal of the substrate evaporation of the solvent or dispersing liquid takes place and a solid layer forms.

A popular model to describe layer thickness for dip-coating processes (Equation 1) was proposed by Landau and Levich in 1942 [33].

$$h_0 = 0.944 \cdot \left(\frac{\mu U}{\sigma}\right)^{\frac{1}{6}} \cdot \left(\frac{\mu U}{\rho g}\right)^{\frac{1}{2}} \qquad (1)$$

According to the model, the layer thickness h_0 is affected by the viscosity of the liquid μ, the withdrawal speed U, the surface tension of the liquid σ, as well as gravity g and the density of the liquid ρ.

2.4.2 Requirements for the deposition liquid in dip coating processes

The liquid media for deposition usually consist of a solvent or a liquid in which either a precursor of the desired material is dissolved or, as it would be the case for powder particles, dispersed.
In a first step a dipping solution or suspension has to be prepared. Points that are not represented in equation 1 but have to be considered nonetheless are as follows.

- Homogeneity
- Stability
- Volatility of the dispersion medium

Homogeneity is required for an even distribution of the fluid on the sample surface. Stability is required for reproducibility of the layers, especially if multiple coating runs are planned. The volatility of the solvent has to be considered as evaporation may change the concentration of the dipping medium over time and therefore it contributes to the points above (homogeneity and stability). A second point is, that the film thickness after deposition is dependent on the evaporation behavior of the liquid.
Surface tension of the dispersion medium has an influence on the wetting of surfaces. The lower the surface tension of the liquid, the more likely a liquid is to wet a surface. Equation 2 (Young-Laplace relation) describes the work of adhesion between a liquid phase and a solid substrate.

$$W_{adh} = \gamma_{LV} + \gamma_{SV} - \gamma_{LS} \qquad (2)$$

γ is the interfacial tension between two phases and L, S or V stand for liquid, solid and vapor phase respectively. For negative values of W_{adh} the liquid spreads over the surface, while for positive values the liquid will form droplets [34].
Additives like surfactants may be used to stabilize the solution or alter its viscosity

Stabilization or organic slurries by silanization

Silicon nitride powder usually has a thin oxide layer on its outer surface and, depending on the environment, silanol groups [35, 36]. This means that it has a polar surface, which makes stabilizing its dispersions in organic, nonpolar solvents highly difficult. One to increase powder interaction with an apolar liquid is by attaching nonpolar groups to its surface.
One approach to do so is through silanization reagents, such as trimethoxysilane compounds. Figure 2 shows 3-Aminopropyltrimethoxysilan as an exemplary silanization agent.

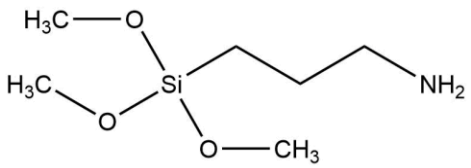

Figure 2: 3-Aminopropyltrimethoxysilane

The compounds are first hydrolyzed, to form silanol groups, which can in turn bind to the powder surface through a condensation reaction with the powder's silanol groups on its surface [37].

2.4.3 Masking of macroporous substrates

To prevent infiltration of the macroporous substrate with the coating fluids the macropores have to be masked [38].

Literature about such masking techniques is scarce, but two different and promising techniques will be described here.

Elyassi et al. [39] have described the use of a highly diluted solution of polystyrene (1 wt%) in toluene. They deposited an intermediate layer from a dispersion of n-hexane, polycarbosilane (PCS) and silicon carbide powder onto their support by slip casting and subsequent pyrolysis of the PCS. A sacrificial interlayer was applied by dipping the samples into the polystyrene solution, followed by the application of the separation layer by dip coating into a solution of n-hexane and PCS. During pyrolysis the sacrificial interlayer was burned out.

Hedlund et al. [40] applied a PMMA film onto commercially available alumina substrates and then immersed the samples in molten wax under vacuum to enhance infiltration. After solidification of the wax the PMMA film was dissolved in acetone. This process takes one week. Following the removal of the PMMA layer the membrane layer was applied by dipping the samples into a solution with seed crystals for hydrothermal synthesis.

3 Experimental Procedure

In the following chapters the production process of the substrates, the masking and the different layers will be described.

3.1 Materials

Table 3 shows a list of the materials used.
The poly(vinyl)silazane (Durazane 1800, Figure 3) was always used with 1 wt% dicumyperoxide as a radical initiator dissolved in it.

Table 3: List of materials used

Name	Formula	Producer	Batch
Silicon nitride SN-XP06	Si_3N_4	Ube Industries Ltd.	Z166210
Silicon nitride SN-XP06	Si_3N_4	Ube Industries Ltd.	Z166Y07
Silicon nitride SN-E10	Si_3N_4	Ube Industries Ltd.	A166610
Alumina CT3000Sg	Al_2O_3	Almatis	1 103323490 0
Yttria AB134554	Y_2O_3	H. C. Starck	09061/06
Dolapix A88		Zschimmer & Schwarz	251804
Durazane 1800	See Figure 3	durXtreme GmbH	IN01100924-13J
Dicumylperoxide	$[C_6H_5C(CH_3)_2]_2O_2$	Fluka	1319051
Polystyrene, atactic (FW 800-5000)		Alfa Aesar	S08B014

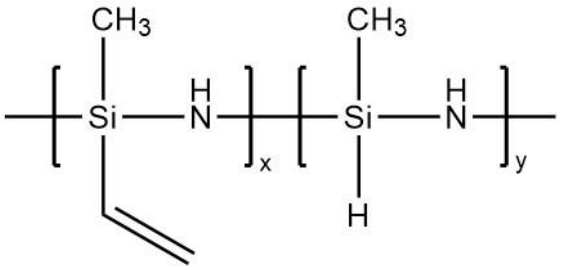

Figure 3: Structure of the preceramic polymer used. x equals 0.2 and y equals 0.8.

3.2 Preparation of tubular Si_3N_4-support structures by slip-casting

The processing steps in the following chapter were optimized by Thomas Prochaska in his master thesis [41]. In chapter 4.1, a comparison between the achieved results is given.

3.2.1 Preparation of aqueous silicon nitride slurries

Aqueous slurries were prepared with the composition given in Table 4. SN-XP06 from UBE Industries was used. In Table 3 are two different batches listed due to the first batch being used up over the process of the work.
As a dispersing agent, Dolapix A88 by Zschimmer & Schwarz was chosen. It is an amino alcohol in solution and is recommended by its producer for the preparation of aqueous silicon nitride slurries. Dolapix A88 and the sintering additives were weighed as one percent in relation to silicon nitride.

Table 4: Composition of an aqueous silicon nitride slurry that was used in slip casting

	Amount (wt%)
Water (deion.)	35.77
Dolapix A88	0.63
Y_2O_3	0.63
Al_2O_3	0.63
Si_3N_4 (SN-XP06)	62.35

For a typical experiment, 34.5 g water were weighed into a 250 ml PE-bottle, followed by 0.6 g of Dolapix A88, Al_2O_3 and Y_2O_3. Then 22 silicon nitride milling balls (½ in diameter) were added. 60 g of silicon nitride powder were added in two steps. After half the powder had been added the ingredients were mixed by thoroughly shaking the bottle. After that the second half of the powder was added the bottle was shaken again, until all the powder appeared to be wet and then the bottle was transferred to a milling table. This was repeated two more times. The bottles remained on the milling table for 20 hours. The milling balls were removed with a sieve. Typically, three bottles were produced per batch that were combined into one bottle after sieving. This bottle was again put onto the milling table until it was needed for further processing.

3.2.2 Rheology of aqueous slurry

The rheological properties of aqueous silicon nitride slurries (composition see Table 4) were analyzed using a modular compact rheometer MCR 300 by Physica Anton Paar. For the measurements a PP25 measuring system (25 mm diameter) was used at a gap of 1 mm and a temperature of 25 °C. The shear rate was steadily increased from 0 to 100 s^{-1} and for the viscosity measurement five values at a shear rate of 100 s^{-1} were determined. Figure 4 shows the test setup.
Two slurries were investigated. One slurry was prepared on the day before the measurement (04/23/2018), while the other slurry was prepared two and a half months earlier (02/13/2018)

and left on the milling table for that timespan. The first slurry was measured four times, whereas the second slurry was measured only three times.

Figure 4: Rheometer used for characterization of the aqueous slurries

3.2.3 Preparing gypsum molds

For slip casting a gypsum mold with high water withdrawal capabilities was needed. The mold was produced in two parts.

The plaster was prepared by combining gypsum (Supraduro, Lehrer Töpferbedarf, 330 g) with water (220 g). After letting it settle for 90 seconds, the mixture was manually stirred for another 110 seconds before shaking the container for the trapped air bubbles to come out. The plaster was then poured into a prepared PP frame that was glued onto a flat glass panel. A PTFE cylinder, which was cut in half along its height, had previously been placed in its center. The mixture was further degassed by manually vibrating the mold for 2 minutes.

After 45 minutes the first half of the mold could be recovered from the casting form and the second half was cast with the same plaster mixture. This time, a full PTFE cylinder was placed into the first half of the mold, the frame was put on top of it, and the half was coated with a separation emulsion before pouring the mixture into the frame again. The mixture was degassed again by vibrating for 2 minutes.

After another 45 minutes the second half could be removed from the casting setup and a pouring funnel was carved into the mold.
The mold was left in a drying cabinet at 55 °C overnight before it could be used for slip casting.

3.2.4 Slip casting

For slip casting the silicon nitride slip was removed from the milling table, a part of it transferred into a different container and degassed in a planetary centrifugal mixer (Thinky ARE-250 CE). The degassing was done in two steps. The container containing the slip was put into the device and degassed at 800 rpm for 10 minutes. The slip was controlled for air bubbles on the surface before degassing for another 10 minutes. After that the slip was poured into the prepared gypsum mold, which was then manually rotated for 70 seconds to ensure a consistent wall thickness. After that the excess slip was poured out of the mold, which was placed upside down onto the table and left for drying overnight. After drying the cast silicon nitride tube was recovered from the mold and dried for at least 24 h in a drying cabinet at 110 °C.
The dried tubes were measured (outer diameter, wall thickness and weight) before sintering.

3.2.5 Sintering of silicon nitride supports

Sintering was carried out in a hot press (FCT HPW 150/200-2200-100-LA), which is depicted in Figure 5.
The base of a graphite crucible was covered in a 1:1 mixture (by weight) of boron nitride and silicon nitride. On top of the powder bed five to six silicon nitride fragments were placed, onto which the tubular supports were placed, which were then covered with silicon nitride fragments. This was to prevent powder from the powder fill from getting inside the tubes and breaking them by shrinkage of the samples during the sintering process.
After covering the tubes with silicon nitride fragments, more powder mixture was put into the graphite crucible until it was completely filled (at which point the tubes were also completely covered).
A graphite lid was placed onto the crucible, which was then put into a graphite mantle. The whole setup was put into the hot press, which was then closed and purged with nitrogen by alternating evacuation (5 minutes) and nitrogen flushing (until ambient pressure) cycles two times.
For consistency evaluation the transferred heat during the sintering process was measured with PTCR Rings (PTCR HTH, Schupp).

Figure 5: Hot press FCT HPW 150/200-2200-100-LA

After purging, the sintering program was started. In the first step the furnace was purged another 3 times with nitrogen. The first two times the pressure was fixed at 450 mbar, whereas for the third step the pressure was fixed at 1050 mbar.
Due to the temperature only being monitored by a pyrometer, the temperature control up to 650 °C was done by limiting the heating power to 4 kW. At 650 °C the temperature control was taken over by the pyrometer and the remainder of the ramp up to 1700 °C was completed with a heating rate of 10 K/min.
The full sintering program is shown in Table 5.
After the first month of working with the hot press the pyrometer was exchanged, due to pyrometer malfunction.
In chapter 4.1, a comparison of samples before and after the pyrometer change is described.

Table 5: Sintering program for the silicon nitride substrates

Step	Relevant parameters
Purging	450 mbar N_2
Purging	450 mbar N_2
Purging	1050 mbar N_2
Heating to 650 °C	Fixed heating power of 4 kW
Heating to 1700 °C	Heating rate 10 K/min (controlled by pyrometer)
Dwelling	5 h
Cooling to 650 °C	10 K/min
Cooling to room temperature	Heating power of 0 kW

3.2.6 Post-processing of the supports

The supports were ultrasonically washed in water and dried before their density (and thus their porosity) was evaluated (see chapter 2.4.2).
After density evaluation the supports were cut to length with a diamond cut-off wheel on a cutting machine (Uniprec Woco 50), ultrasonically washed, degreased with acetone and dried again at 110 °C.

3.2.7 Characterization of the supports

Porosity and permeability were chosen to characterize the tubular support structures and were compared to results obtained in previous works.

Porosity determination following EN 623-2

Standard DIN EN 623-2 [42] describes the density and porosity measurement of porous ceramics by water immersion. This analysis was performed on the heat-treated samples.
After drying the samples at 110 °C overnight, their dry weight (m_1) was determined. The samples were then placed on a rack in a desiccator with a funnel and a valve on top and a three-way valve connecting to a membrane vacuum pump and the environment. See Figure 8 for a schematic of the apparatus used. The rack is necessary to ensure that no bubbles are caught inside the tubes, when they are immersed.
The funnel (valve closed) was filled with water and vacuum was applied (less than 25 mbar) for 15 minutes, after which the valve to the pump was closed and the upper valve was opened. The samples were immersed in water in a way that at least 2 cm of water was above them. It is important not to let the funnel run dry, since this would introduce air into the system.
After filling the apparatus with water the valve to the funnel was closed and vacuum (less than 25 mbar) was applied for another 30 minutes. Then the system was vented and the samples were left in the water for another 30 minutes.
Next the samples were, one by one, removed and characterized by measuring the weight under water (m_2) three times and the weight after wiping them with a wet, fuzz-free towel to remove excess water and the samples were weighed three times in air with water trapped in their pores (m_3).
According to the standard geometric bulk density (ρ_b), apparent density (ρ_s) and apparent porosity (Π_a) were calculated.

$$\rho_b = \frac{m_1}{m_3 - m_2} \cdot \rho_L \qquad (3)$$

$$\rho_s = \frac{m_1}{m_1 - m_2} \cdot \rho_L \qquad (4)$$

$$\Pi_a = \frac{m_3 - m_1}{m_3 - m_2} \cdot 100 \qquad (5)$$

Permeability

The permeability of the supports was tested by measuring the gas flow through tubular samples at different pressures. For most of the sintering batches one tube was characterized. The test rig is a modified version of a test rig used in DIN EN ISO 4022 [43]. In the standard procedure only planar samples can be measured, however by using custom fittings and a sealed steel capsule it is possible to test tubular samples. Figure 6 shows a schematic of the apparatus.

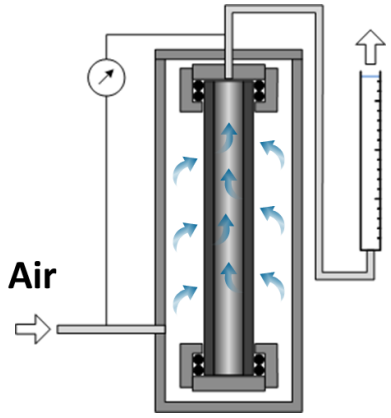

Figure 6: Schematic of the permeability test rig [44].

Before testing, the samples were to be dried at 110 °C overnight. After cooling down two rubber O-rings were slid over one end of the sample and the tube was sealed by screwing nut into a screwcap. On the other side a nut was placed on the tube and again two rubber O-rings were slid over the tube. The tube was screwed onto the lid of the steel capsule, then the lid was placed on top of the capsule and sealed with a clamping ring.

The air flow through the samples at different pressures was measured using a soap bubble flow meter. The differential pressure was increased from 0.2 to 1.0 bar in 0.2 bar increments and from 1.0 to 3.0 bar in 0.5 bar increments. At the different pressure differentials, the flow was measured using a soap bubble flowmeter. The time it took the compressed air to fill a known volume was taken. Using Forchheimers equation (equation 6) it is possible to determine Darcian (k_1) and Non-Darcian (k_2) permeabilities [45].

$$\frac{p_i^2 - p_0^2}{2p_0 \cdot l} = \frac{\eta}{k_1} \cdot \frac{Q}{A} + \frac{\rho}{k_2} \cdot \left(\frac{Q}{A}\right)^2 \qquad (6)$$

By fitting a quadratic function of $\frac{Q}{A}$ vs. $\frac{p_i^2 - p_0^2}{2p_0 \cdot l}$, using the method of least squares, the coefficients $\frac{\eta}{k_1}$ and $\frac{\rho}{k_2}$ were calculated and used to determine k_1 and k_2.

k_1 was chosen as relevant parameter when comparing the prepared samples to samples from former works.

3.3 Coating of tubular supports

The tubular supports were to be coated with either an intermediate layer, composed of silicon nitride powder and a poly(vinyl)silazane derived component, that should act as a binder and a separation layer composed of only poly(vinyl)silazane derived ceramic or directly with the separation layer.

The coating process can be divided into several steps which are shown in the flow diagram in Figure 7. Only the principles of the different steps will be described in this chapter. A detailed overview of all the samples and their production steps and parameters for the coating process can be found in Table 6, Table 7 and Table 8 for masking of the substrate, direct application of separation layer, and intermediate layer application, respectively.

Table 6: Overview over the experiments conducted on the masking of the substrates. The numbers in brackets mean (withdrawal speed; holding time) for the dip coating process and (Imm) indicates that the samples were masked by immersion.

	Sintering run	Pre-treatment	Masking
M_2_EPS5	2	no	EPS5 (Imm)
M_2_EPS25	3	no	EPS25 (Imm)
M_2_EPS36	3	no	EPS36 (Imm)
M_4_EPS15_140;1	4	no	EPS15 (140;1)
M_1_EPS25_20;5_PT	1	yes	EPS25 (20;5)
M_7_EPS25_20;5_PT	7	yes	EPS25 (20;5)
M_4_Wax	4	no	Wax
M_8_PS25_20;5	8	no	PS25 (20;5)
M_1_EPS25_20;60_PTFE	1	PTFE-wrap	EPS25 (20;60)
M_3_PS25_20;60_PTFE	3	PTFE-wrap	PS25 (20;60)

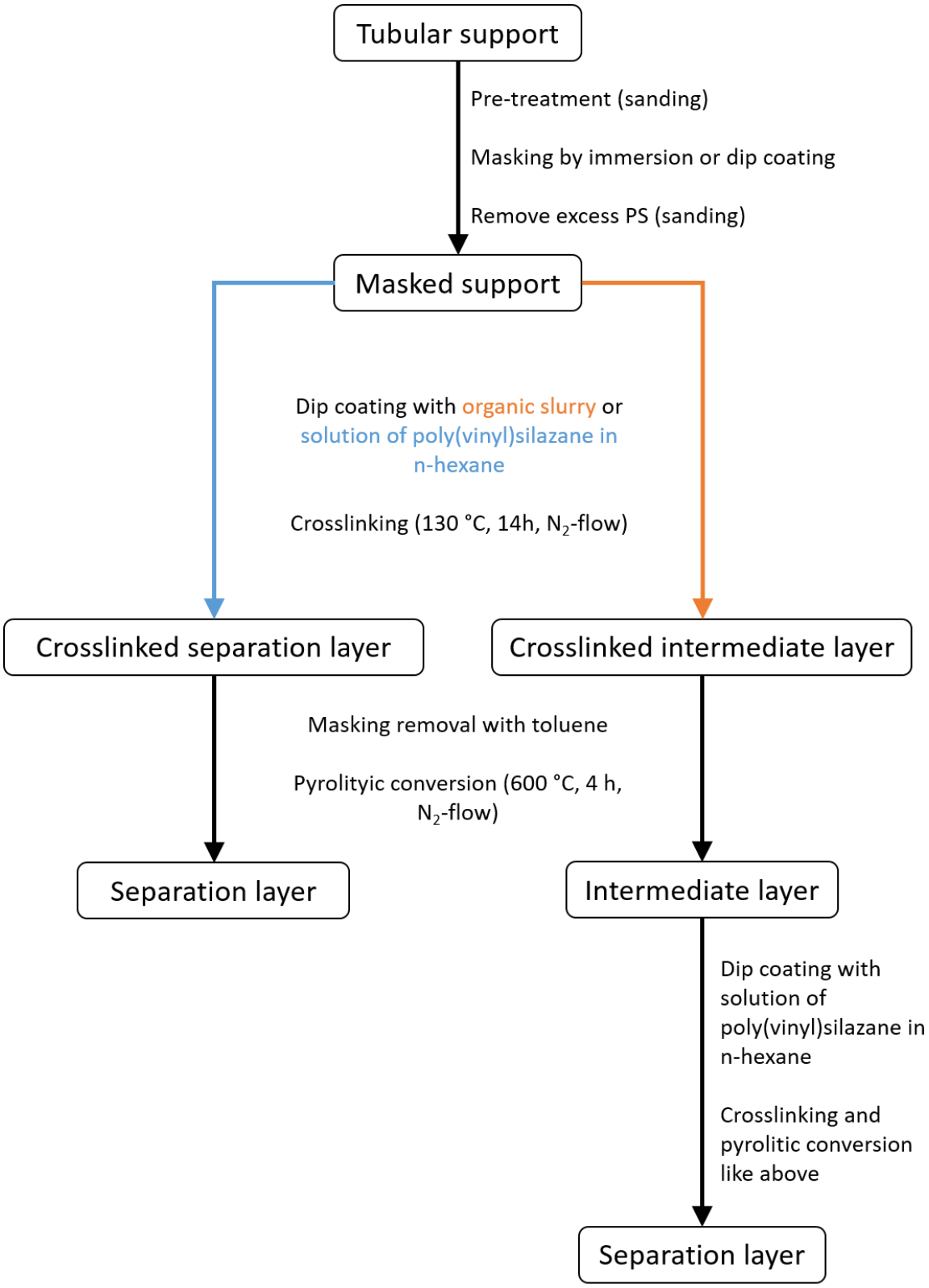

Figure 7: Flow diagram of the coating process

Table 7: Overview over experiments on direct coating of the masked supports with the separation layer. The numbers in brackets mean (withdrawal speed; holding time) for the dip coating process (Imm) indicates that masking was carried out by immersion.

Sample	Sintering run	Pre-treatment	Masking	Layer	Toluene
D_2I_140;1	2	no	EPS36 (Imm)	PSZDCP (140;1)	no
D_2J_140;1	2	no	EPS25 (Imm)	PSZDCP (140;1)	no
D_3G_120;1	3	no	EPS36 (Imm)	PSZDCP (120;1)	no
D_3G_140;1	3	no	EPS36 (Imm)	PSZDCP (140;1)	no
D_3F_120;1	3	no	EPS25 (Imm)	PSZDCP (120;1)	no
D_3F_140;1	3	no	EPS25 (Imm)	PSZDCP (140;1)	no
D_3H_140;1	3	no	EPS25 (140;1)	PSZDCP (140;1)	yes
D_3I_140;1	3	no	EPS36 (140;1)	PSZDCP (140;1)	yes
D_6H_20;1	6	no	EPS25 (20;1)	PSZDCP (20;1)	yes
D_7A_20;1	7	no	EPS25 (20;1)	PSZDCP (20;1)	yes
D_8A_20;1	8	no	EPS25 (20;1)	PSZDCP (20;1)	yes
D_6J_20;1_IC (Inside coating)	6	no	no	PSZDCP (20;1)	yes

Table 8: Overview over experiments on intermediate layer application. The numbers in brackets mean (withdrawal speed; holding time) for the dip coating process.

Sample	Sintering run	Pre-treatment	Masking 1	Layer 1	Toluene	Post-treatment	Masking 2	Layer 2	Toluene 2	Note
IL_Int1_140;1	4	no	EPS25 (140;1)	Int1 (140;1)	no					
IL_Int1_140;1_NoMask	4	no	no	Int1 (140;1)	no					
IL_70A_140;1	5	no	EPS25 (140;1)	70A (140;1)	yes					
IL_80A_140;1	5	no	EPS25 (140;1)	80A (140;1)	yes					
IL_90A_140;1	5	no	EPS25 (140;1)	90A (140;1)	yes					
IL_70B_20;5	8	yes	EPS25 (20;5)	70B (20;5)	yes	marking	EPS25 (20;5)	PSZDCP (20;5), PSZDCP (140;1)	yes	
IL_80B_20;1	7	yes	EPS25 (20;5)	80B (20;1)	yes					
IL_90B_20;5	8	yes	EPS25 (20;5)	90B (20;5)	yes	no	no	PSZDCP (140;1), PSZDCP (140;5)	yes	
IL_80A_20;1	7	no	EPS25 (20;1)	80A (20;1)	yes	no	no	PSZDCP (20;1)	yes	
IL_80C_20;1	7	no	EPS25 (20;1)	80C (20;1)	yes	no	no	PSZDCP (20;1)	yes	
IL_80B_20;1_2	6	yes	EPS25 (20;5)	80B (20;1)	yes					Delamination, no further coatings possible
IL_80B_20;5	6	yes	EPS25 (20;5)	80B (20;5)	yes					
IL_80B_140;5	8	yes	EPS25 (20;5)	80B (140;5)	yes					
IL_80B_20;1_3	8	no	EPS25 (20;1)	80B (20;1)	yes					
IL_80B_20;1_4	8	no	EPS25 (20;1)	80B (20;1)	yes					

3.3.1 Pretreatment of supports

The supports that were cut to length were either directly used for coating or sanded with silicon carbide paper (p320, p600 and p2000). The sanding is necessary to eliminate scratches or imperfections stemming from either slightly damaged plaster molds or from the handling of the very fragile green bodies. If sanding or polishing steps were involved in the production of samples, it is indicated in the tables above by a “yes” in the column “Pre-treatment”.
After the surface treatment the supports had to be cleaned. The cleaning was done in an ultrasonic bath in three steps, each time for 10 minutes. For the first two steps the samples were placed in a beaker with water and for the last step they were degreased with acetone.

3.3.2 Masking of tubular supports

To prevent infiltration of the substrate’s pores they had to be masked.
Previous experiences had shown that polystyrene is best suited as masking material, since it leaves the least residue in the pores after being removed during pyrolysis [46].
As a masking liquid solutions of different concentrations of polystyrene dissolved in toluene were investigated. The polystyrene was in most cases EPS (packaging material), however a commercially available polystyrene from Alfa Aesar with a molecular weight in the range of 800 to 5000 g/mol was also used in later stages of the work. The samples for which this was used are specifically labelled with “PS25” instead of “EPS25” in Table 6.

In a first step, masking by infiltration was tested. The samples were put into an infiltration apparatus (see Figure 8), which was then evacuated to 100 mbar pressure. The masking liquid was then poured over the samples until they were completely covered. After 15 more minutes at 100 mbar the pressure was adjusted to ambient and the samples were removed from the liquid.

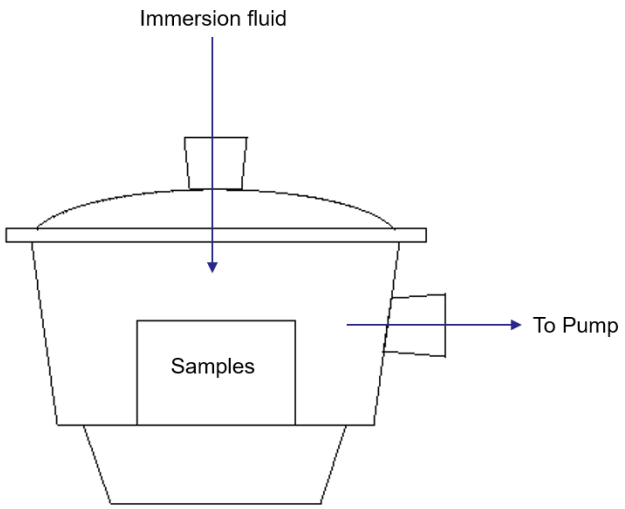

Figure 8: Schematic of the infiltration apparatus. The immersion fluid was put into a funnel that could be cut off from the apparatus with a valve.

In a second step, masking by dip coating into the solution was also investigated. The support tubes were mounted onto an arm, which was moved by a stepper motor. Figure 9 shows the setup.

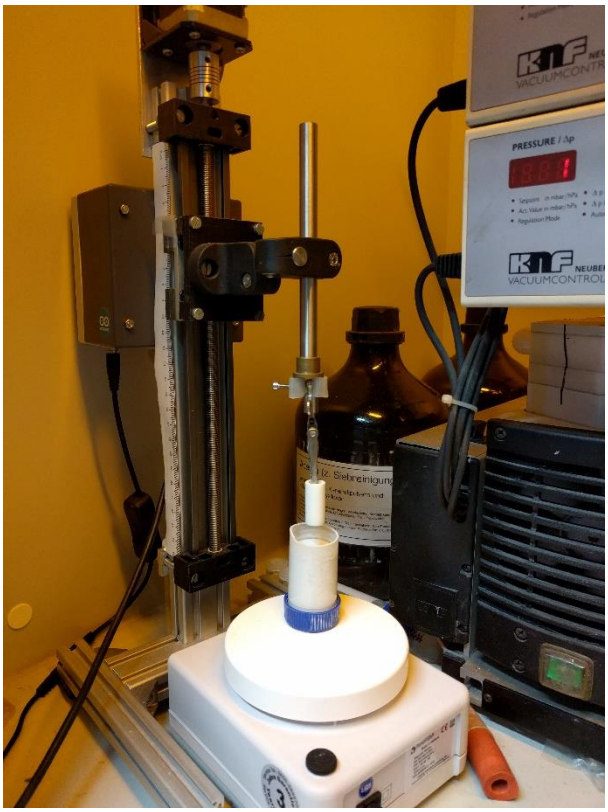

Figure 9: Dip coating setup

Dipping parameters such as dipping velocity, holding time (in solution/slurry), and withdrawal speed could be specified in the control program.
The masked supports were dried in a drying cabinet at 110 °C for at least two hours. The masking with viscous EPS solutions left a dense PS film on the surface of the supports. This excess masking on the outside of the tubes was removed by grinding and polishing with silicon carbide paper (p320, p600 and p2000). Whether enough material had been removed was checked by scratching the tubes with a spatula. On the excess polystyrene masking no visible markings could be made, whereas on the silicon nitride scratch lines were clearly visible. This method proved to be non-sufficient in later tests, which is why later samples were marked before coating by abrading a spatula on the surface of polished tubes and then coating them with the masking solution. The coating was sanded until the markings were starting to get lighter from grinding, which was chosen as the point at which higher grits up to 2000 were used. As soon as the markings were completely gone the polishing was stopped. Figure 10 shows samples that were marked before masking after the application of the masking by dip

coating. Pens and sharpies were also tested to mark the surface of the supports, but the ink/dye was pulled into the substrate through capillary effect.
After surface treatment by grinding, the supports were again ultrasonically cleaned.

Figure 10: Samples that were marked and then masked. Excess PS is still present.

Alternative masking methods:

As alternatives to the masking and polishing method it was also investigated whether the outside of the tubes could be wrapped with PTFE tape, so that no masking-film would cover the whole surface of the supports but solution would still infiltrate the whole sample from its inside.
Supports that were wrapped with PTFE band were dip coated with either EPS or PS solutions.

3.3.3 Application of intermediate layer by dip coating

The steps involved in preparing the deposition liquid and coating the samples will be described below.

Preparation of organic slurry for intermediate layer application

As intermediate layer a mixture of silicon nitride (SN-E10, UBE) and poly(vinyl)silazane (Durazane 1800, durXtreme GmbH) in an organic solvent was chosen. The organic solvent had to meet the following criteria:

- Must result in a stable suspension with silicon nitride powder
- Must not dissolve polystyrene
- Must not react with poly(vinyl)silazane

Different compositions, solvents, and additives were investigated, since - as stated in chapter 2.4.2 - the stability of the coating liquid is crucial for achieving homogenous surfaces. Table 9 shows different slurries that were investigated.
The first slurry produced (Int1) was used for preliminary tests only and was based on a slurry used in a previous work of the research group [46].
Subsequently, two different solvents were investigated. 2-Butanone is a solvent that is very commonly used in the preparation of tape casting slurries. Duan et al. [47] have used it in an azeotropic mixture with ethanol. However, since evaporation properties are not as crucial for the purpose of this work and since ethanol would react with the preceramic polymer, it was assumed that 2-Butanone (methyl ethyl ketone) alone would suffice. After preparing the first batch of samples however, it was discovered that the ketone reacted with the preceramic polymer as well as it would dissolve the masking, and thus it was not suitable as a solvent. If 2-butanone was used as solvent, it is indicated in Table 9.
n-Hexane does not react with the preceramic polymer and does not dissolve polystyrene, so it was used in almost all of the experiments. Since n-hexane was used for most samples its usage is not indicated in Table 9
Furthermore, it was investigated whether or not drying the powder or using oleic acid as dispersing agent would increase the slurry stability.
The nomenclature of the slurries can be explained by correlating the number with the percentage (by weight) of organic solvent in the slurry, whereas the letter stands for the ratio of silicon nitride powder to preceramic polymer (A - 3:1, B - 1:1, C -1:3). OA indicates the addition of oleic acid to the slurry, while MEK indicates the substitution of n-hexane as solvent with 2-butanone.
The slurries were prepared by combining the components and 20 silicon nitride milling balls (5/16 in diameter) in PE bottles and then putting them on a milling table for at least 20 hours.

Table 9: Compositions of different organic slurries that were investigated

Slurry	Silicon nitride (wt%)	Poly(vinyl)silazane (wt%)	Solvent content (wt%)	Notes
Int1	5.503	4.127	90.4	
70A	22.5	7.5	70	
70B	15.0	15.0	70	
70C	7.5	22.5	70	
80A	15	5	80	
80B	10	10	80	
80C	5	15	80	
90A	7.5	2.5	90	
90B	5	5	90	
90C	2.5	7.5	90	
80A_dry	15	5	80	Powder dried at 300 °C for 3h
80A_OA	15	5	80	Oleic Acid (0.5 %)
80C_OA	5	15	80	Oleic Acid (0.5 %)
80A_MEK	15	5	80	2-butanone as solvent
80C_MEK	5	15	80	2-butanone as solvent

Since no stable slurries could be achieved with the compositions mentioned above, a different approach was chosen.
Silicon nitride has an oxide-layer on its grains and as such is very polar, which makes dispersing it in nonpolar solvents virtually impossible.
By silanisation nonpolar groups can be applied to the surface of the powder particles. The following silanisation agents were investigated.

- 3-Aminopropyltrimethoxysilane
- Allyltrimethoxysilane
- Isobutyltrimethoxysilane
- Propyltrimethoxysilane

The process was based on a guide by Gelest Inc. [48].
The necessary amount of silane can be calculated with the following equation 7.

$$Silane\ (g) = \frac{Si_3N_4\ (g) \cdot specific\ surface\ area\ (\frac{m^2}{g})}{specific\ wetting\ surface\ of\ silane\ (\frac{m^2}{g})} \qquad (7)$$

The specific surface area of the silicon nitride powder used (E10) was 11.1 m²/g, according to the data sheet of the material.
The specific wetting surface of the different silanes were taken directly from a suppliers' homepage (www.gelest.com).

The silane was hydrolysed by mixing with a solution of 5 vol% water (deionized) in ethanol in a way that it would result in a 2 wt% solution of the silane in the alcohol/water solvent. For all silanes except for 3-Aminopropyltrimethoxysilane (because of the amine group), the pH of the alcohol/water mixture was adjusted to 4.5 to 5 with acetic acid.
After hydrolyzing the silane for 5 minutes the silicon nitride was added and the suspension was stirred for another 10 minutes. The container was then put into an ultrasonic bath for 3 minutes before it was stirred again for 1 minute. This process was repeated three times, before centrifuging the suspension, discarding excess solution and washing two times with ethanol. The powder was dried at 110 °C in a drying cabinet before further usage in slurry preparation. See Table 10 for the compositions of the prepared slurries.

Table 10: Compositions of organic slurries that were prepared using surface modified powders.

Slurry	Silicon nitride (wt%)	Poly(vinyl)silazane (wt%)	Solvent content (wt%)	Notes
80A_sil1	15	5	80	3-Aminopropyltrimethoxysilane
80A_sil2	15	5	80	Allyltrimethoxysilane
80A_sil3	15	5	80	Isobutyltrimethoxysilane
80A_sil4	15	5	80	Propyltrimethoxysilane

Sedimentation behavior of organic slurries

To investigate the stability of the organic slurries with which the intermediate layer was supposed to be applied, their sedimentation behavior was measured.
The slurry was taken directly from the milling table and poured straight into a test tube (approx. 15 mL). The starting liquid level was marked, which is essential since evaporation of the solvent must be taken into account. Then every 5 minutes the level of the solids was marked until 30 minutes had passed. The slurry was then discarded and pictures (with scale) of the test tubes were taken (see Figure 11). For evaluation the relative level of the solids content at given times were plotted (see Figure 12 for an exemplary plot).

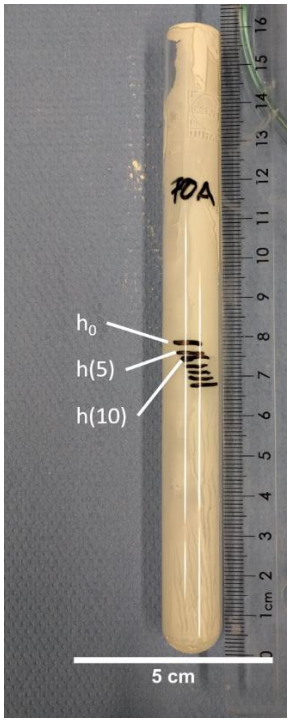

Figure 11: Test tube after sedimentation testing

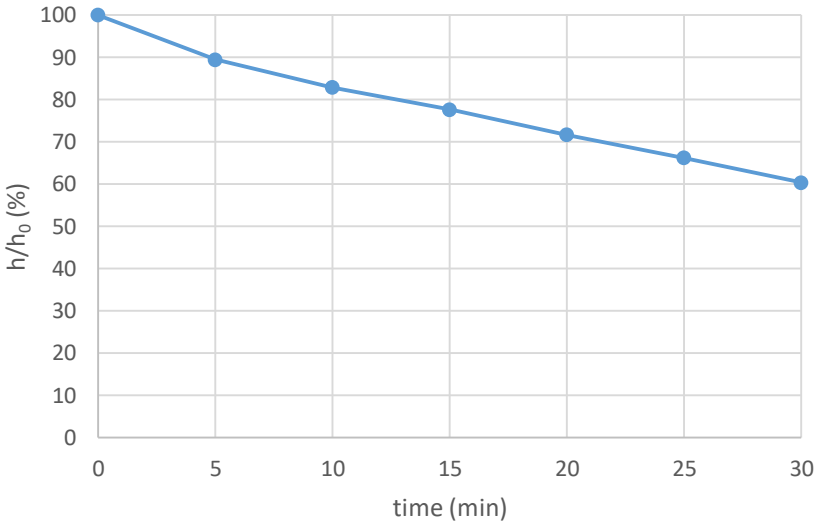

Figure 12: Exemplary plot of sedimentation tests. h/h_0 is the ratio of the level of solid contents in the slurry divided by the initial liquid level

Deposition and heat treatment of intermediate layer

Since no stable dispersions could be achieved with any of the methods, it was decided to magnetically stir the slurries for the entire dip coating process, which was carried out using the same set up as used for the masking.

Only the preliminary tests, which are indicated in Table 8 with “Int1” in the column “Layer 1”, were carried out without stirring the coating liquid.

After dip coating, the preceramic polymer was crosslinked in a furnace at 130 °C for 14 h (ramp: 1 K/min, Nitrogen flow of 0.3 L/min).

In the first few experiments the masking was burned out during the pyrolysis step. It was later found that this may damage the coating’s integrity and as such it was decided to dissolve the masking in toluene after crosslinking the preceramic polymer (which makes it insoluble in toluene). The tubes were placed in a beaker and covered with toluene. To prevent damage to the layer structure the solvent was not stirred but the tubes were manually moved to disturb the solvent (“yes” in the column “toluene” in Table 7 and Table 8 indicates that this procedure was applied).

After 30 minutes in toluene the tubes were dried at 130 °C under a nitrogen flow of 0.3 L/min and pyrolyzed following the heating profile shown in Figure 13, also under a nitrogen flow of 0.3 L/min.

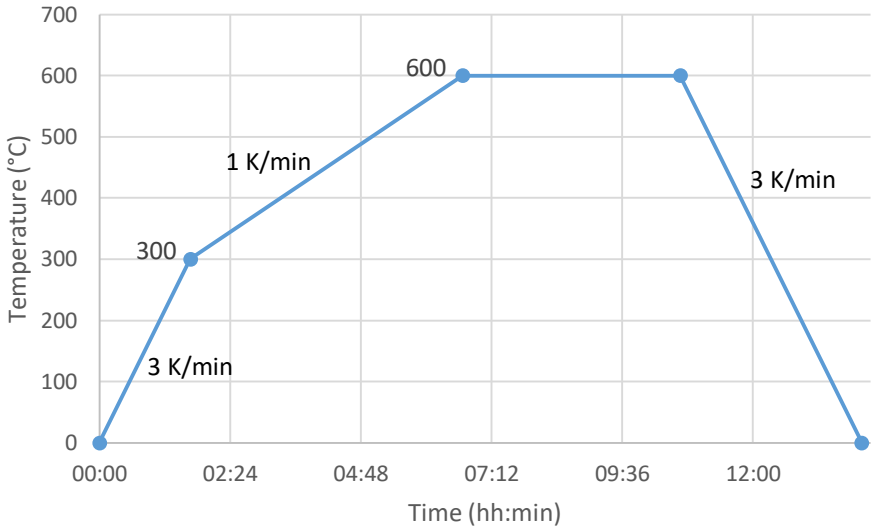

Figure 13: Temperature program for the pyrolysis of the coated samples

3.3.4 Deposition and heat treatment of separation layer

A solution of 50 vol% poly(vinyl)silazane, containing 1 wt% dicumylperoxide with respect to poly(vinyl)silazane, in n-hexane was chosen as the dipping liquid for the separation layer.
The separation layer was applied in two different ways, either onto the intermediate layer or onto the masked support tubes without an intermediate layer.

Deposition of separation layer onto intermediate layer

The separation layer was applied onto the intermediate layer by dip coating.
It was investigated whether or not masking the intermediate layer was necessary to achieve a homogenous surface by preparing samples with and without masking. However, only a limited number of samples could be produced as the intermediate layers were often times very inhomogenous. Table 8 lists the samples produced.

Deposition directly onto masked supports

The dip coating procedure was the same as the one used for applying the separation layer onto the intermediate layer. For details on the produced samples refer to Table 7.

Coating on inner tube surface

The inside of the support tubes after slip casting is exceptionally smooth and does not show any significant damage like cracks, which is why it was also investigated if the membrane layers could be applied onto the inside of the support tubes.
The coating process was only slightly altered for applying inside layers. The outer surfaces of the tubes were wrapped with PTFE tape before dipping them into the solution.
Since there was no practical way found to remove the masking on the inside of the tubes they were not masked before applying the inside coating. Only one sample was suitable for further investigation. It was not masked and did not have an intermediate layer applied prior to dip

coating into a solution of n-hexane in toluene (1:1) with a withdrawal speed of 20 mm/min and a holding time of 1 second.

Heat-treatment of samples

The separation layer was treated the same way as the intermediate layer, by crosslinking at 130 °C for 14h (ramp: 1 K/min, Nitrogen flow of 0.3 L/min) and then pyrolyzed at 600 °C under nitrogen flow of 0.3 L/min (see Figure 13) in a tube furnace.

3.4 Morphology characterization of the masking and layers

Secondary electron microscopy was performed on surfaces and fracture surfaces of the samples after most of the production steps to observe the morphology of the deposited maskings and layers.

Slices of the samples were cut off with a cutting machine (Uniprec Woco 50) and then manually broken into pieces. The fracture surface, as well as the inner and outer surfaces of the samples were analyzed.

The samples were attached onto sample holders using double-sided carbon adhesive tape. In order to prevent electrostatic charges, the samples were sputtered with gold using a sputter coater by Agar and then also contacted with conductive paint (containing Ag).

The micrographs were taken on a Quanta 200 by FEI. All micrographs of coated samples were taken after pyrolysis of the preceramic polymer if not stated otherwise.

4 Results

The following chapters feature the results of the conducted experiments.

4.1 Tubular supports

In this chapter all results concerning the production of the tubular supports will be shown.

4.1.1 Rheology of aqueous slurries

The rheological properties of two slurries were tested. The aim of this analysis was to investigate the storage stability of the slurries. Figure 14 shows shear stress against shear rate. Shear rate was cut off for values below 40 s^{-1} because of irreproducible results possibly due to drying of the slurry on the edges of the plate and solidifying. Thus a solid layer had to be broken, resulting in higher shear stress.

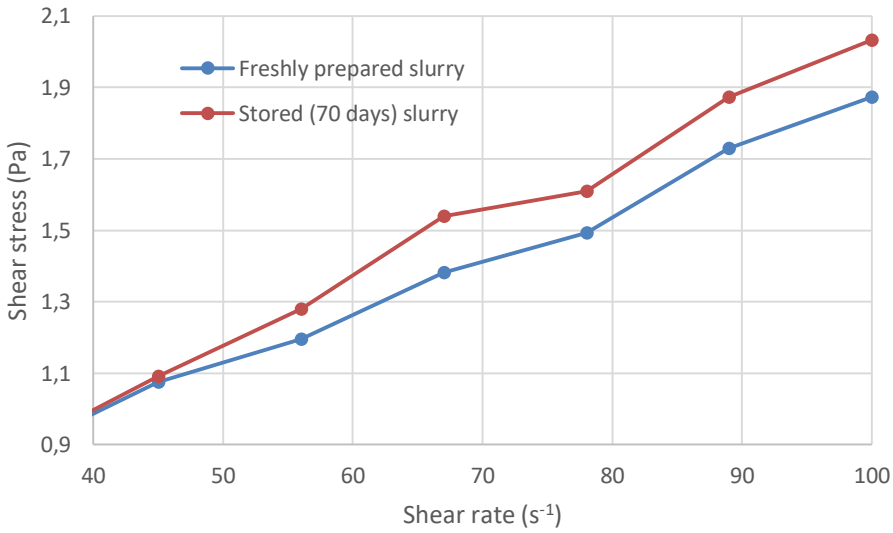

Figure 14: Results of the rheological characterization. The graphs show the average shear stresses of the two slurries against shear rate.

Figure 15 shows the averages of the viscosity measurements of the two slurries.

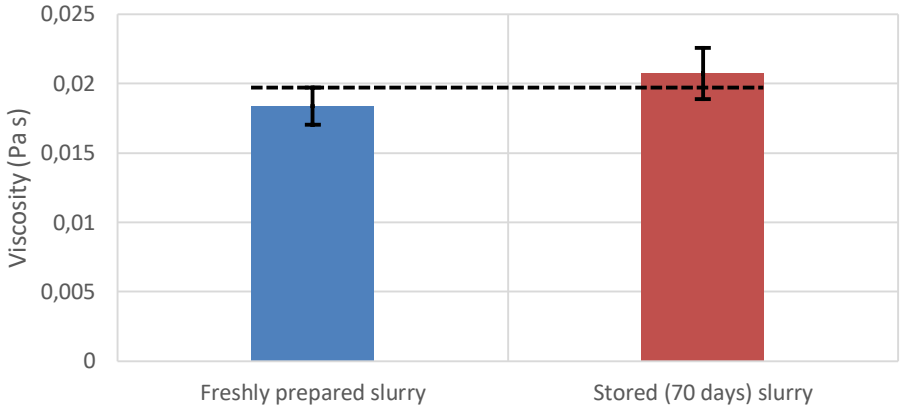

Figure 15: Comparison of the viscosity of the two aqueous slurries. The dashed line is only a visual aid.

4.1.2 Porosity of tubular supports

Figure 16 shows the results of the porosity determinations. The porosity was correlated with the heating power of the hot press at the dwelling temperature, since the temperature was always supposed to be at 1700 °C but due to the old pyrometer being defective the power draw would always be different. The samples produced using the old pyrometer are shown in blue. For all samples sintered with 9.0 to 9.1 kW the new pyrometer was used (green data points).

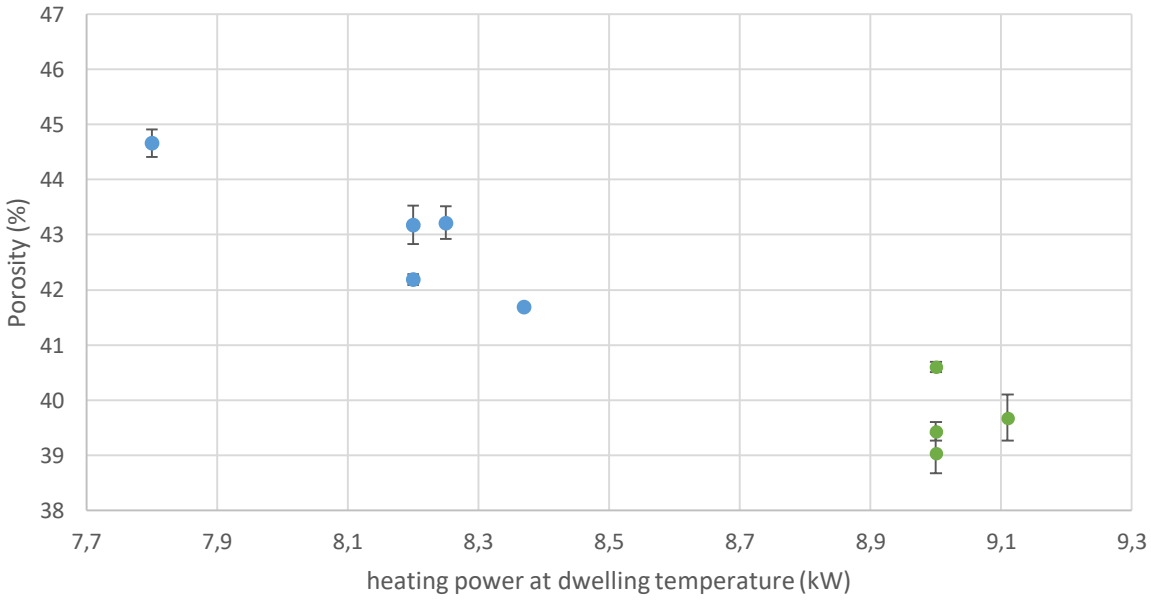

Figure 16: Results of the porosity determinations by immersion. The dots represent the averages of the respective sintering runs. Samples represented in blue were sintered using the old pyrometer, whereas samples represented by green data points were sintered using the new pyrometer.

4.1.3 Permeability of tubular supports

Figure 17 shows the results of the investigation of the permeability of the samples correlated with the sample porosity, whereas Figure 18 shows the correlation with the heating power of the hot press at the holding temperature. Data points represent samples prepared with the old pyrometer (blue) and the new pyrometer (green).

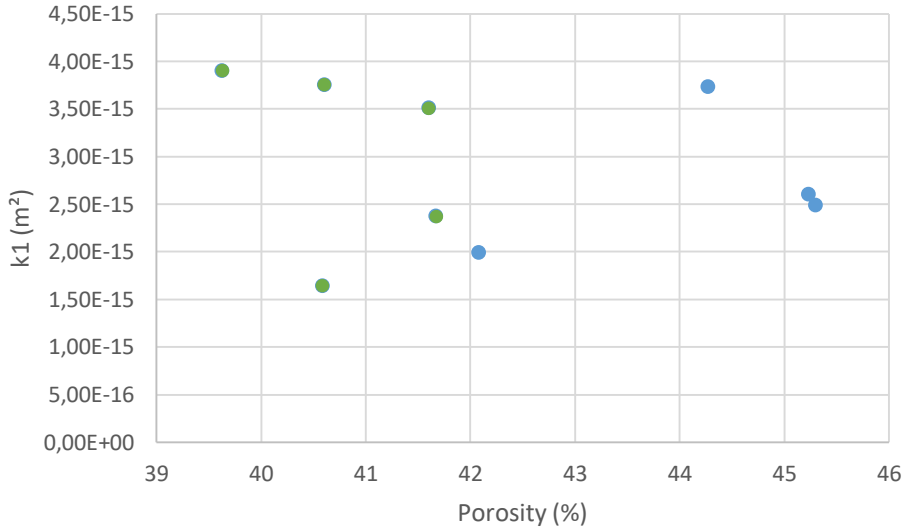

Figure 17: Darcian permeability plotted against porosity. Represented in green are samples that were sintered using the old pyrometer, whereas blue data points show results of samples sintered using the new pyrometer.

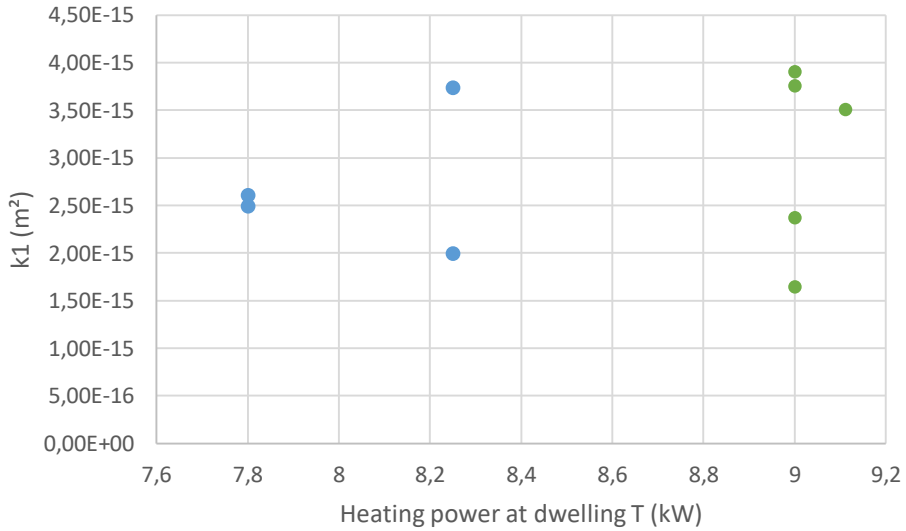

Figure 18: Darcian permeability plotted against the heating power of the hot press during the dwelling period of the sintering process. Blue shows samples sintered using the old and green using the new pyrometer.

4.2 Assessment of the masking procedure

The quality of the masking was investigated by SEM.

4.2.1 Effect of EPS-solution concentration on coating morphology

Figure 19 shows a comparison of the fracture surfaces of four different samples that were masked by immersion in differently concentrated masking solutions. It can be seen that the sample masked with the 5 wt% and 15 wt% solutions do not show significant filling of the pores, whereas the 25 wt% and 36 wt% solutions lead to filled pores as well as a dense polystyrene film on the outer surface layer. It was clear, that the film would have to be removed before coating the samples with the actual membrane layers. The sample masked with an 15 wt% EPS-solution was dip coated, whereas the other samples were masked by immersion. However, results shown in chapter 4.2.2 confirm that the samples may still be compared, since dip coating and immersion lead to comparable masking results.

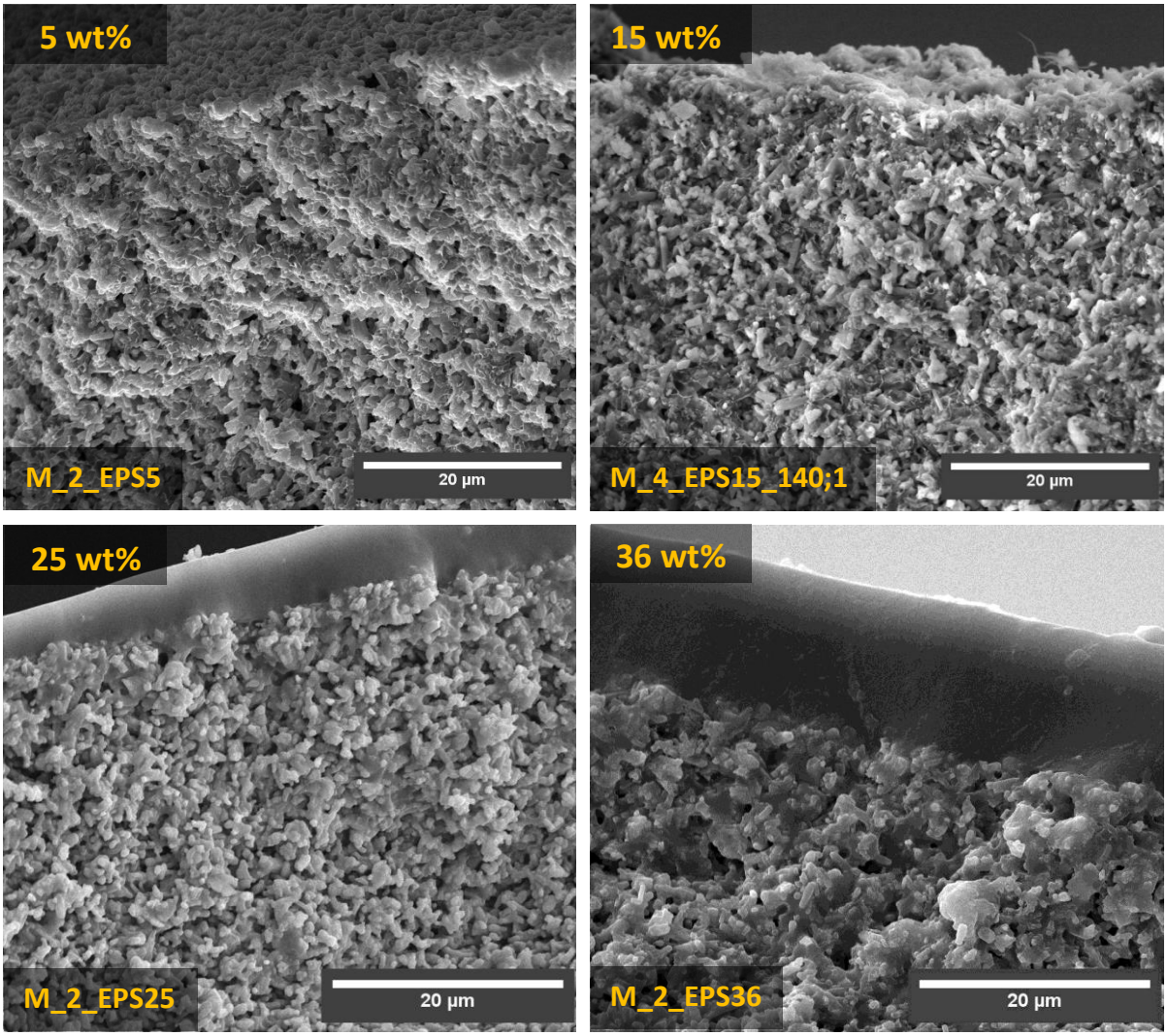

Figure 19: Comparison of samples masked with masking solutions of different concentrations.

4.2.2 Effect of coating method on masking morphology

Two different approaches for the masking procedure were chosen, one was masking by immersion of the samples under lowered pressure, and the other by dip coating. (See chapter 3.3.2 for the detailed descriptions.)

Figure 20 shows a comparative set of micrographs of the fracture surfaces of two samples masked with 25 wt% EPS-solution. The left sample was masked by immersion and the right sample by dip coating. One can identify the outer surface by looking at the dense PS-film, which is located on the surface of the substrates.

It can be seen that the infiltration of the pores of the dip coated sample is comparable to the immersion sample.

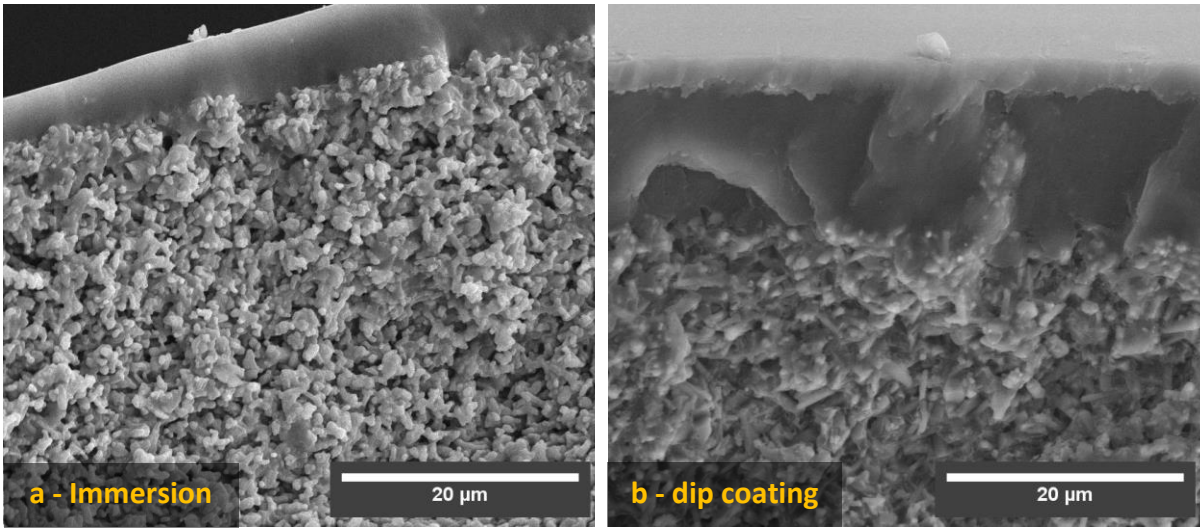

Figure 20: Comparison masking by immersion (Sample M_2_EPS25) or dip coating (M_1_EPS25_20;5_PT)

4.2.3 Effect of masking agent on masking morphology

The following samples were prepared with masking solutions with the same concentration but different polystyrene types (EPS or PS respectively). It can be seen that the sample masked with the PS solution shows that, although most pores are filled, there are still some pores that are not filled. Another difference is that the surface structures are not masked at all (Figure 21).

Masked with EPS (25 wt%) in toluene

Masked with PS (25 wt%) in toluene

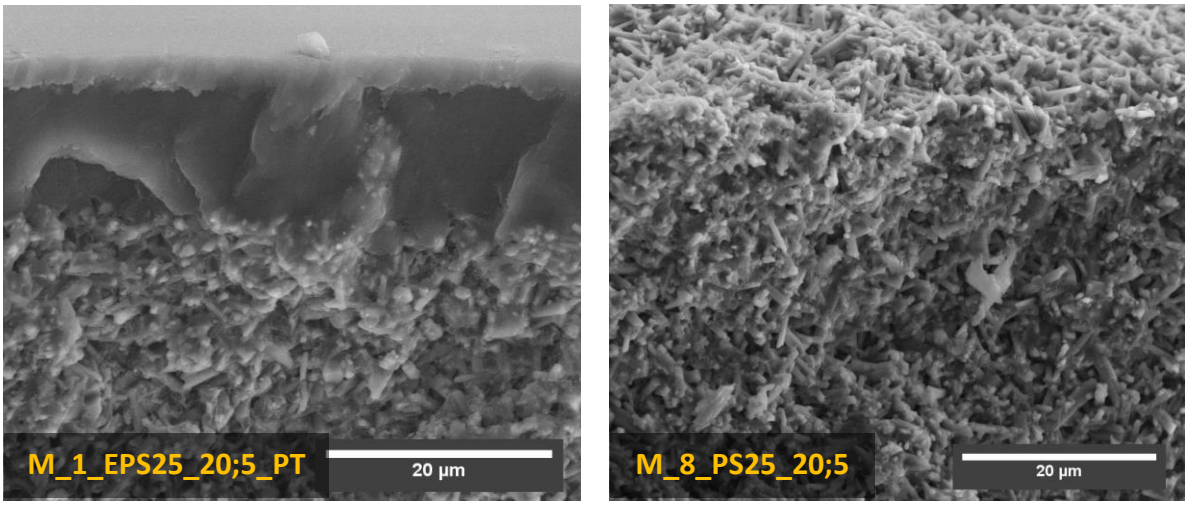

Figure 21: Comparison masking by dip coating with EPS- or PS-solutions

4.2.4 Surface defects of the substrate and their effect on the masking

Sanding and polishing the substrate surfaces generally enhances coating quality. However, not all defects can be removed. Deep grooves may remain on the surface. Figure 22 shows a masked substrate, on which the excess PS has already been removed. There is a deep grove which is still filled with PS. This will result in a defect in the deposited layer after removal of the PS through toluene or pyrolysis.

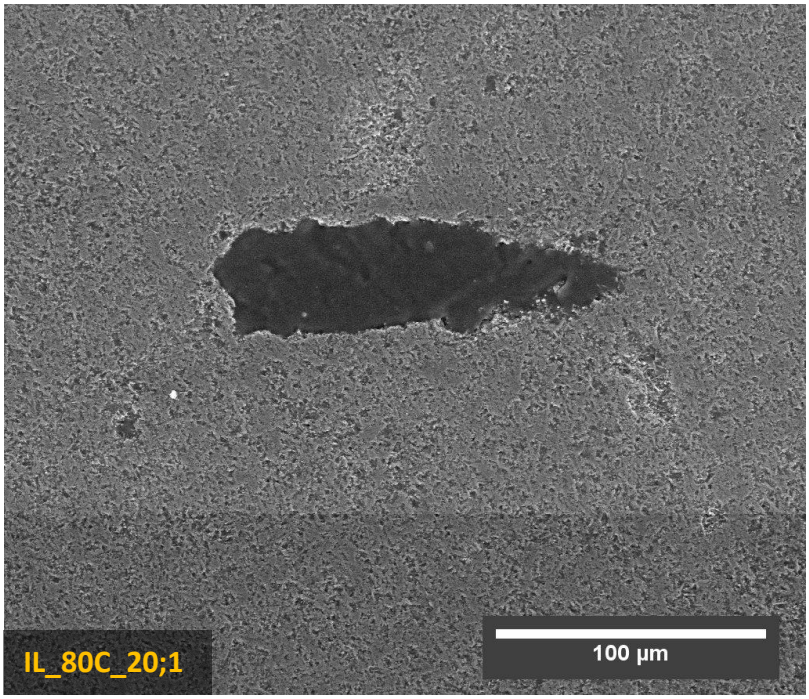

Figure 22: Deep groove on sample surface, after removal of excess masking. The groove is still filled with PS.

4.2.5 Alternative masking methods

The investigated alternative masking methods through infiltration of PTFE wrapped samples with EPS- or PS solution did not yield any usable results, since the infiltration depth was insufficient.

4.3 General observations during coating with different deposition liquids

General observations that were made during the dip coating processes will be described here. The observations concern both – intermediate layer and separation layer – coatings.

Insufficient wetting of deposition fluid on samples

It was observed that some samples were not sufficiently wetted by the deposition fluids. This was the case for the masking solution, the organic slurry, as well as the deposition fluid for the separation layer. It was not until very late in the progress of the thesis that this was spotted, since it can only be seen by different reflection behaviors on the surface of the substrates.

Delamination after pyrolysis

Pyrolysis would often lead to delamination of layers. This was the case for the intermediate layers as well as the separation layers, especially for thick layers. Figure 23 shows an example of delamination of the intermediate layer on samples after pyrolysis.

Figure 23: Delamination of intermediate layers after pyrolysis

4.4 Deposition and morphology of the intermediate layer

The following chapters show all obtained results that are relevant for either intermediate layer deposition or the morphology of the intermediate layers.

4.4.1 Sedimentation of organic slurries

For clarification, the following nomenclature was chosen:
Example 80A: 80 means that this slurry consists of 80 wt% solvent, while A means that three parts of the remaining 20 wt% consist of silicon nitride and 1 part poly(vinyl)silazane. B means 1:1 and C means 1:3.
Figure 24 shows a comparison of sedimentation plots of organic slurries that were prepared with different compositions of silicon nitride, poly(vinyl)silazane and n-hexane. It can be seen that the slurry stability is indirectly proportional to both the amount of solvent and the amount of poly(vinyl)silazane.

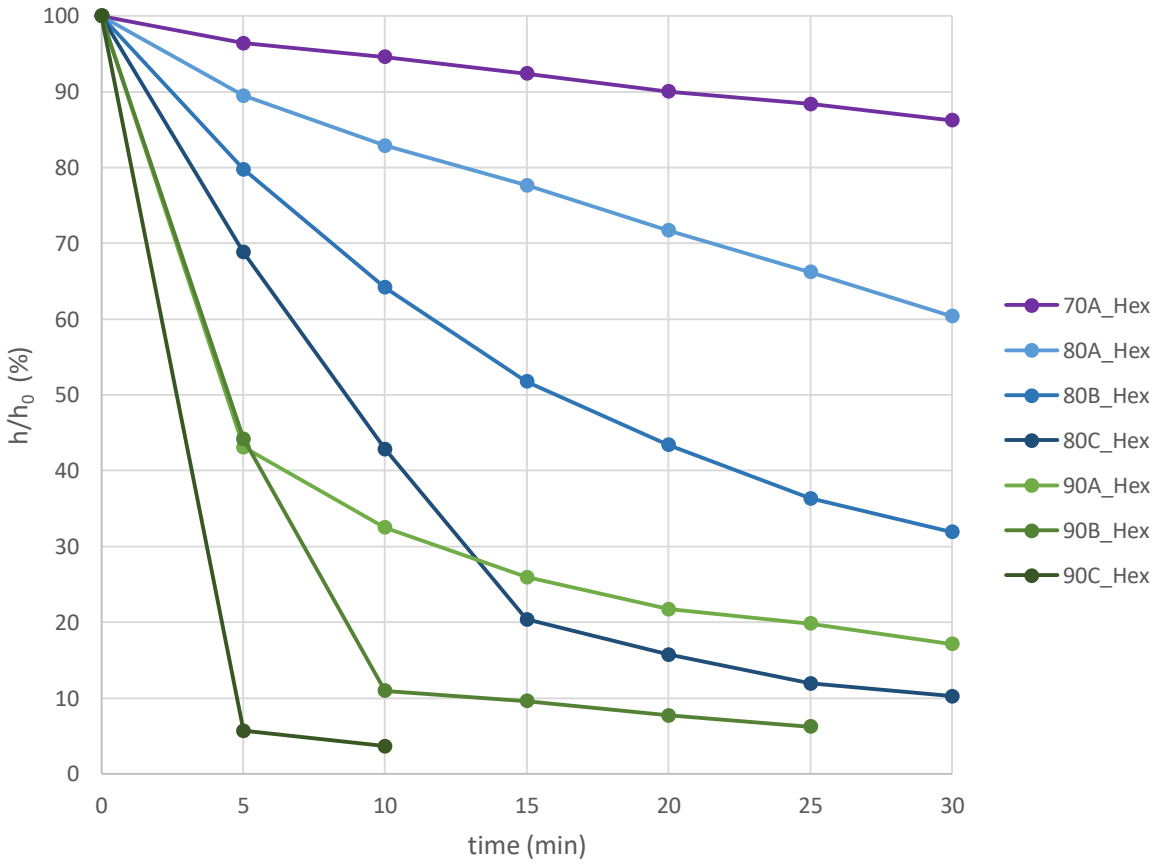

Figure 24: Sedimentation plots of organic slurries with different compositions

In Figure 25, the red graph shows the sedimentation behavior of powder that had been dried prior to slurry preparation, whereas the orange line shows the sedimentation of a slurry to which oleic acid had been added. Both slurries were prepared with an 80A composition. They show no significant change in sedimentation behavior compared to the reference 80A slurry (light blue).
The green line shows an 80A slurry prepared with 2-butanone. This slurry did not show any signs of sedimentation, neither during the 30 minutes of the test nor after 4 more hours of waiting.
The yellow line shows an 80C slurry to which oleic acid had been added. Its stability has been increased significantly compared to the reference, but not enough to be usable. The dark blue line represents an 80C slurry that has been prepared using 2-butanone, which sediments very quickly in the first five minutes but is more stable than the reference (light gray) after that time.

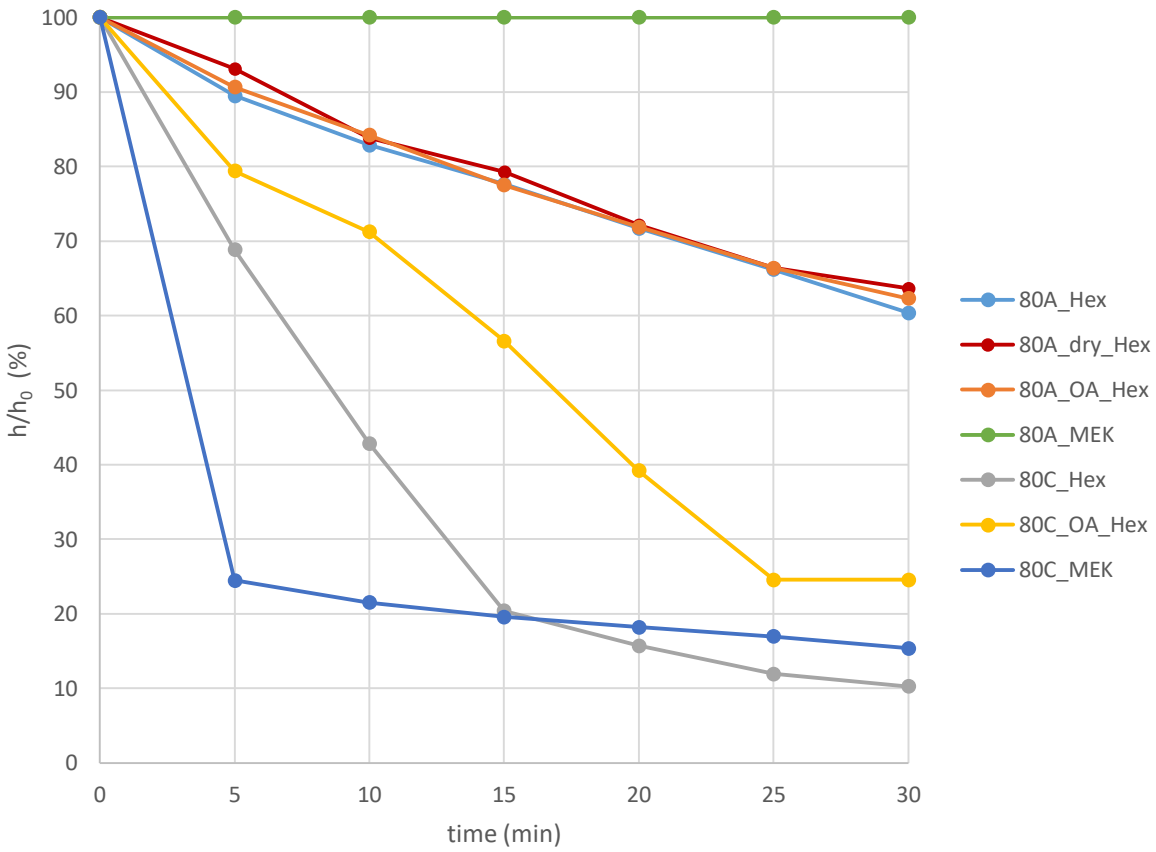

Figure 25: Sedimentation plots of organic slurries prepared with either dried powder, oleic acid or 2-butanone.

Figure 26 shows the results of the sedimentation tests with slurries of 80A composition, that were prepared by using silanised powder. On the right side the silanisation agents used are displayed in the color matching the respective graph. The light blue line is a reference 80A slurry. No significant increase in slurry stability can be found and the powder modified with 3-Aminopropyltrimethoxysilan even shows a higher tendency to sediment.

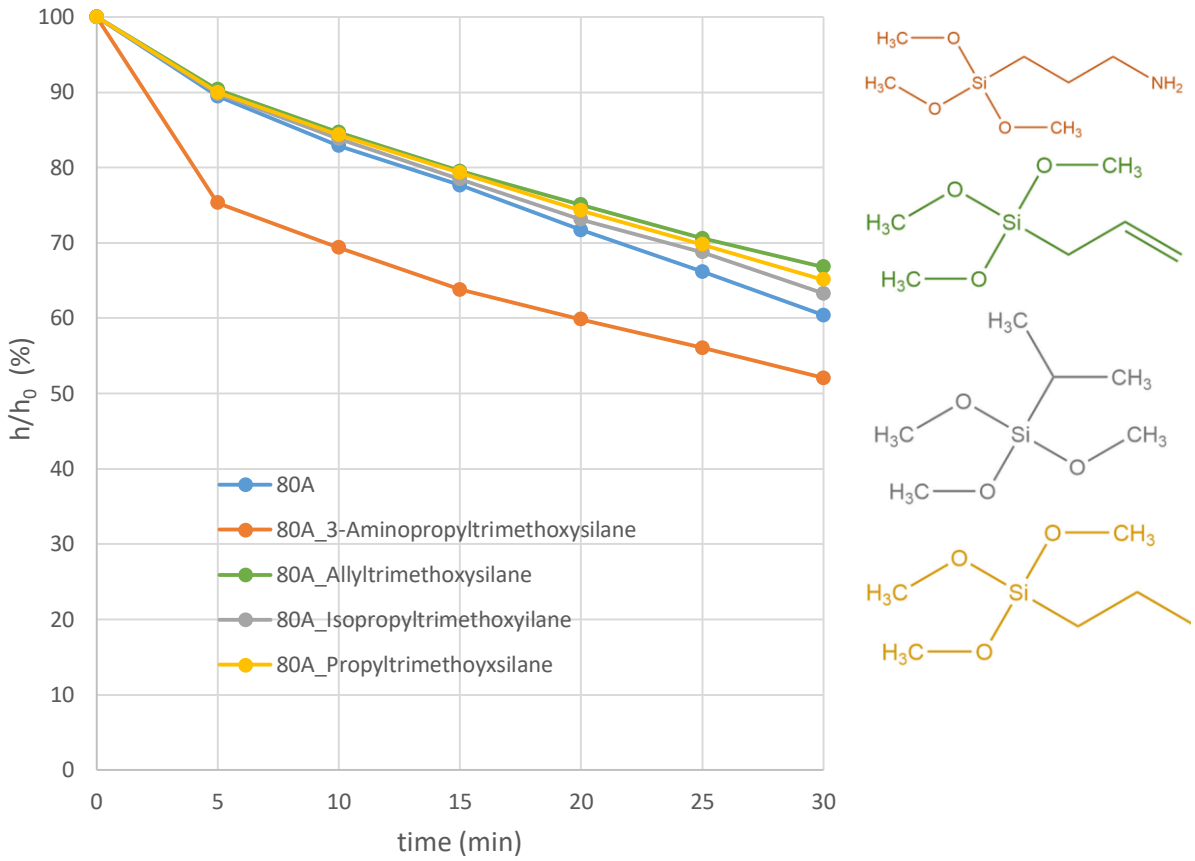

Figure 26: Sedimentation-plots of organic slurries prepared with surface modified silicon nitride powder.

4.4.2 Morphology of the intermediate layer

In the following chapters the morphology of the intermediate layers will be shown in comparative SEM micrographs. Table 11 gives an overview over obtained layer thicknesses.

Table 11: Overview of thicknesses of the obtained intermediate layers on different samples after pyrolysis

Sample	Withdrawal speed (mm/min)	Solvent content (wt%)	Ratio of Si_3N_4 to PSZ	Layer thickness after pyrolysis (µm)
IL_Int140;1	140	80	5:4	9
IL_Int1_140;1	140	80	5:4	17
IL_70A_140;1	140	70	3:1	10
IL_80A_140;1	140	80	3:1	n.a.
IL_90A_140;1	140	90	3:1	30
IL_80A_20;1	20	80	3:1	3
IL_70B_20;5	20	70	1:1	4.5
IL_80B_20;1	20	80	1:1	3.4
IL_90b_20;5	20	90	1:1	3.4
IL_80B_20;1	20	80	1:1	4
IL-80C_20;1	20	80	1:3	5.4

Preliminary tests

Sample IL_Int1_140;1 was produced in a preliminary test. Using a slurry composition (“Int1” in Table 9) from a previous work of the research group the prepared sample (masked and polished afterwards) was dipped into the slurry. However, during the dipping process the solids in the slurry started sinking and as such the whole process was not reproducible

Figure 27a shows a fracture surface before pyrolysis. This micrograph shows the masked substrate and an 18 µm thick intermediate layer with a smooth surface.

Figure 27b shows a fracture surface after pyrolysis. It can be seen that the intermediate layer is much thinner than before pyrolysis. The right side of the micrograph shows a spot where the deposition fluid infiltrated the sample. The surface also appears much rougher after pyrolysis. The outer surface of the sample showed brighter and darker spots if investigated with smaller magnification. Figure 27c shows a higher magnification of a border between the light and dark zones. The right side of the micrograph shows an intact intermediate layer surface, while the left side shows an uncovered substrate surface.

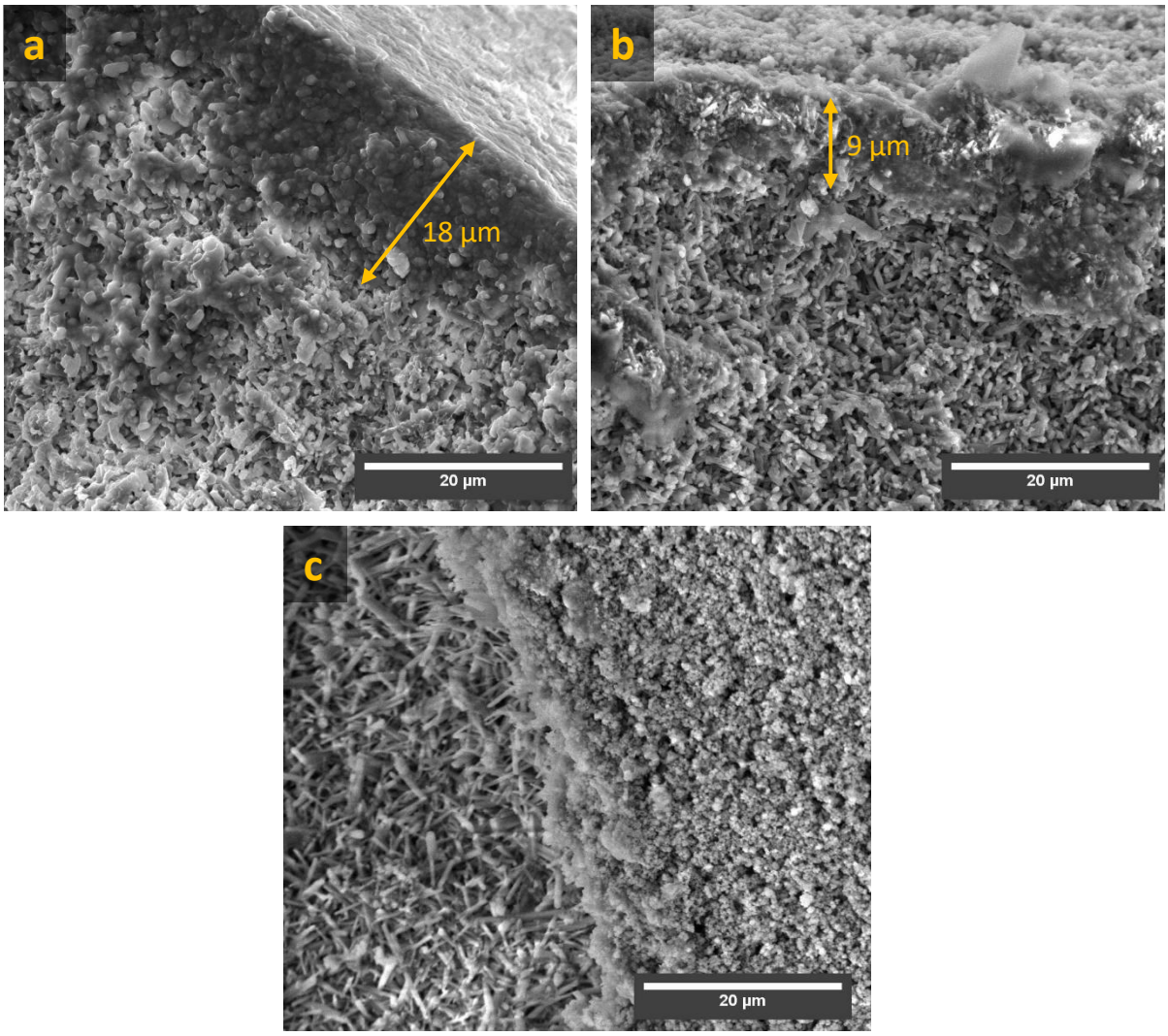

Figure 27: Intermediate layer of sample IL_Int1_140;1, which was prepared in a preliminary test. a shows a fracture surface after crosslinking, b shows a fracture surface after pyrolysis and c shows the outer surface after pyrolysis.

Sample "IL_Int1_140;1_NoMask" was not masked, but rather directly dipped into the organic slurry, resulting in a slip-casting-like process. The porous substrate pulled in the liquid components of the suspension and left behind a thick layer of compacted silicon nitride powder on its surface. This surface layer did not adhere to the surface and either delaminated before or after pyrolysis. A micrograph (Figure 28) of the fracture surface shows that the liquid components of the deposition fluid have infiltrated the substrate. 17 µm from the surface there is a seemingly dense layer with rod-like β-Si_3N_4 poking through. This layer breaks up more and more the deeper the substrate was infiltrated.

The surface of this sample is covered with silicon nitride powder, which might just be leftovers from the layer that peeled off. There are also some needle-like silicon nitride crystals from the substrate which do not seem to have been covered by preceramic polymer.

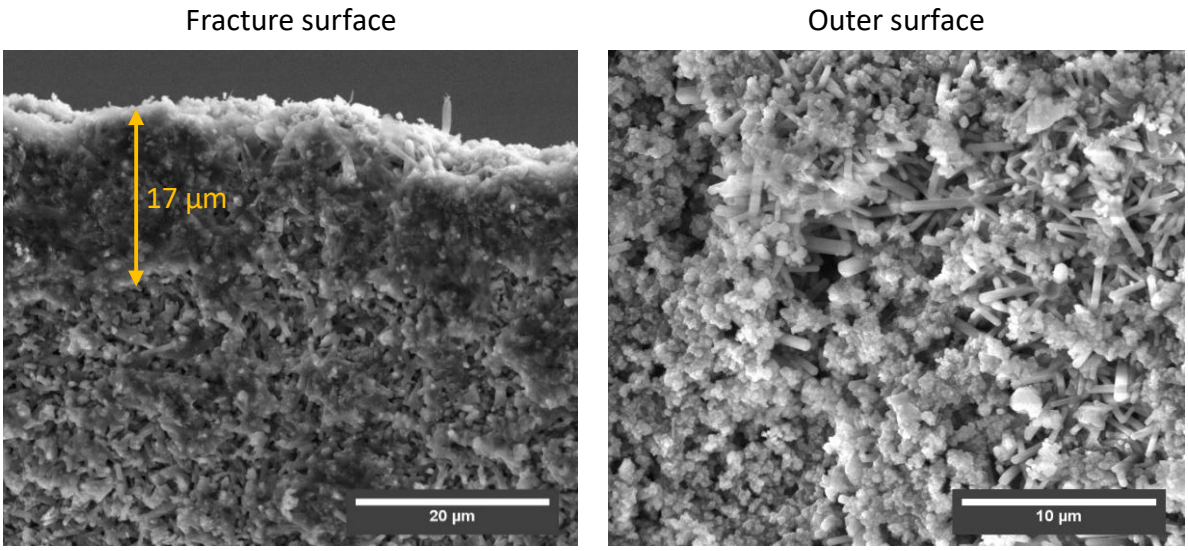

Figure 28: Unmasked sample (IL_Int1_140;1_NoMask) coated with an intermediate layer in a preliminary test.

Effect of solvent content of an organic slurry with A composition on layer morphology

Figure 29 shows comparative micrographs of samples onto which an intermediate layer was applied by dipping into organic slurries with A composition (3:1 silicon nitride to poly(vinyl)silazane), holding for 1 second and withdrawing with 140 mm/min. The solvent content of the organic slurries was varied for the samples, while the ratio of silicon nitride to preceramic polymer was kept constant.

The micrographs in the left column show fracture surfaces after the crosslinking of the polymers. The right column shows the fracture surfaces after pyrolysis of the polymers.

The 80A sample shows a significantly thicker layer (not fully shown on the micrograph). When measured in other micrographs it was 100 µm thick for the crosslinked sample. For the pyrolyzed sample it could not be measured, since it showed a smooth transition between layer and substrate.

The layer thickness decreases for all samples during pyrolysis. All samples show some form of infiltration into the substrate. If sample 80A is treated as an outlier (probably due to slip-casting like behavior due to defective masking) then sample coated with the 90A slurry shows the thickest layer even though the layer was produced with the least concentrated deposition fluid.

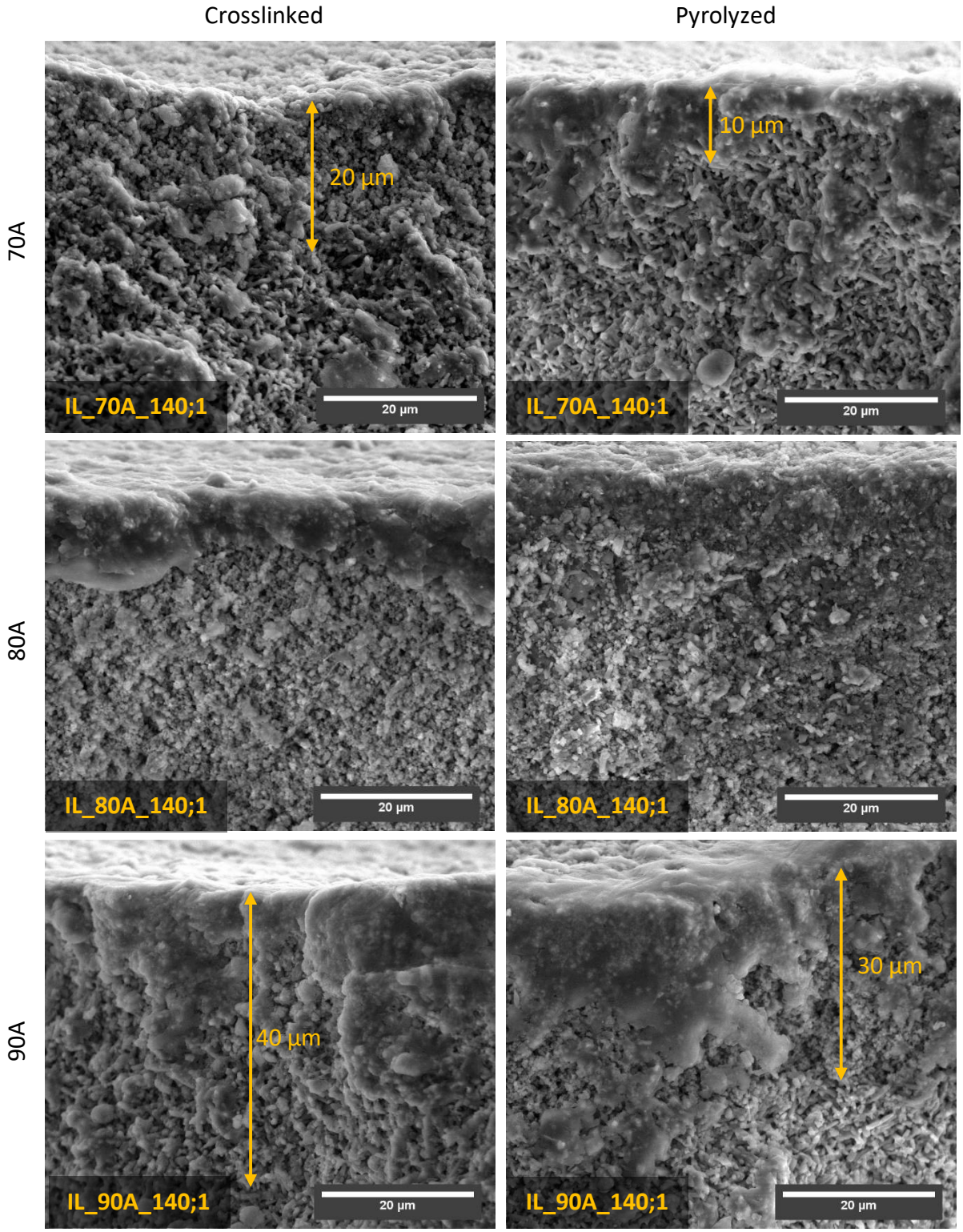

Figure 29: Comparison of samples coated with organic slurries with different solvent contents

The intermediate layer applied with a 90A organic slurry shows another interesting feature in some parts of its fracture surface. Figure 30 shows delamination between the substrate and

the pyrolyzed intermediate layer on a microscopic scale. This is an indicator that this sample also experienced slip-casting-like behavior during the dip coating process.

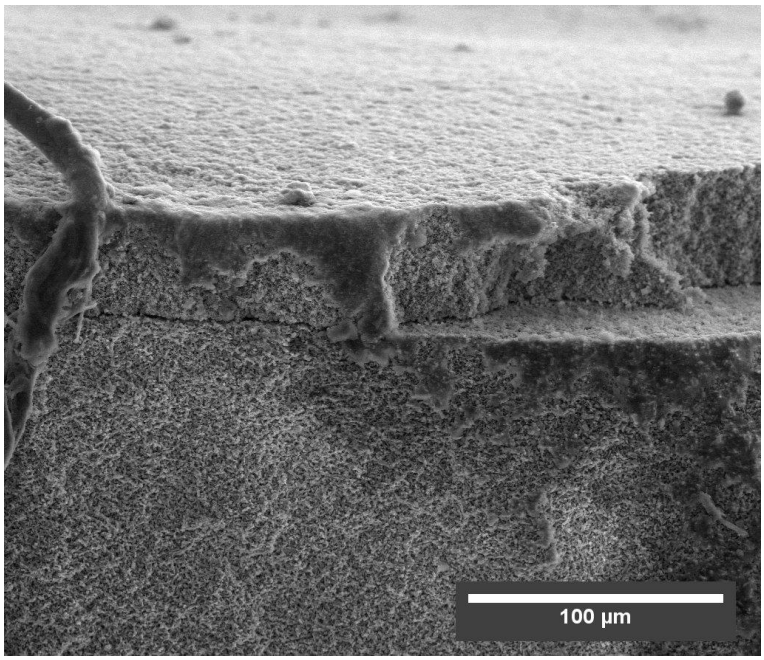

Figure 30: Delamination of a sample IL_90A_140;1

Effect of solvent content in organic slurry with B composition on layer morphology

Figure 31 shows a comparative set of micrographs of samples prepared with an organic slurry with a B ratio (1:1 silicon nitride to poly(vinyl)silazane) using different solvent contents. The withdrawal speed for the dip coating of these samples was kept at 20 mm/min. No significant difference in layer thickness between different solvent contents was observed. The samples coated with 70B and 90B show incomplete coverage of their surfaces. The sample coated with the 80B slurry shows partially good coverage together with parts of the surface that are not covered at all.

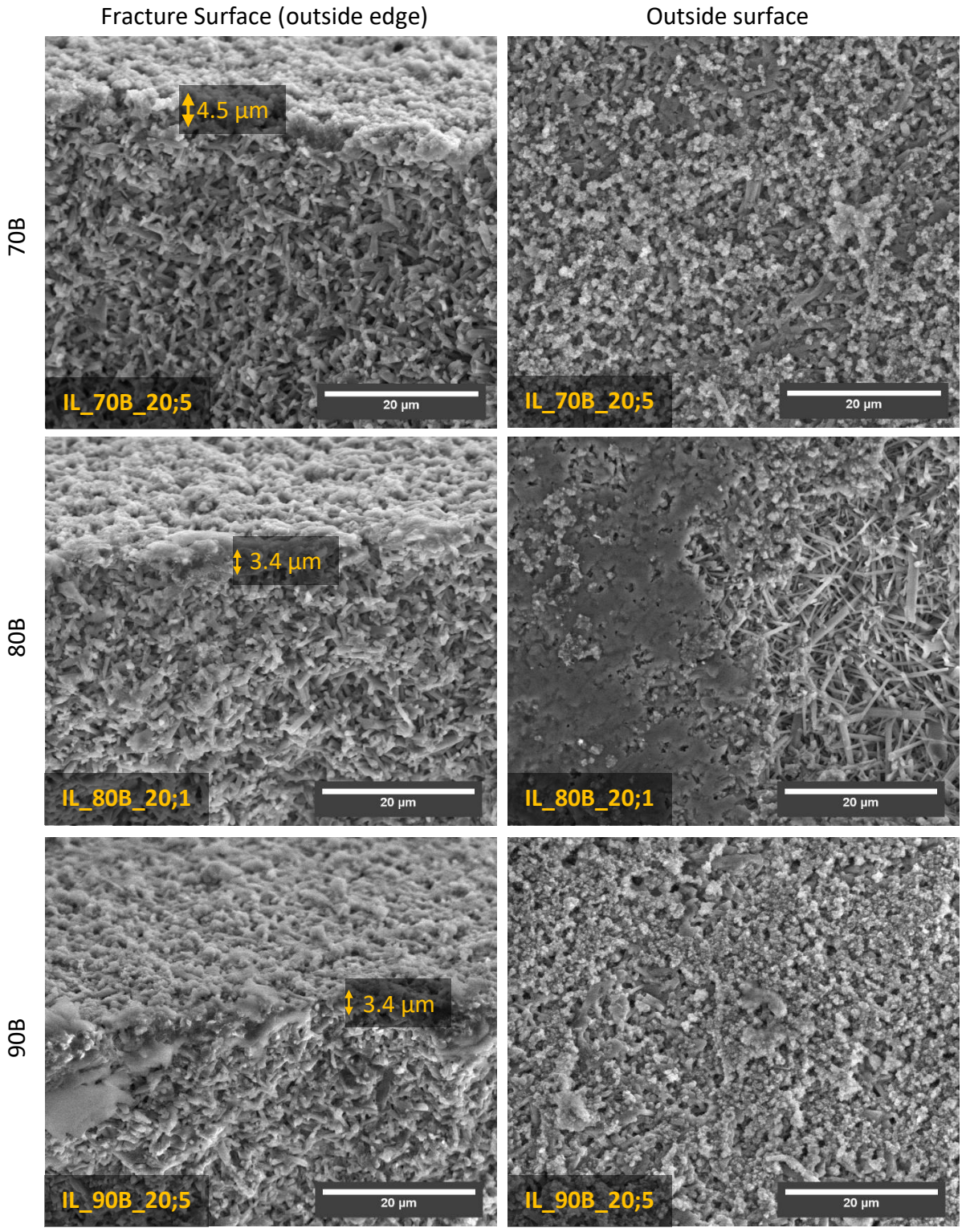

Figure 31: Comparison of samples coated with organic slurries of B composition but varying solvent contents

Effect of ratio of Si_3N_4 to PSZ in an organic slurry with 80 wt% solvent on layer structure

The following Figure 32 shows a comparison of pyrolyzed samples coated with organic slurries consisting of 80 wt% n-hexane but different ratios of silicon nitride powder to preceramic polymer. All samples were polished before masking, which shows a significant increase in surface quality.

The layers on all samples are relatively thin (compared to Figure 29), which might be due to the low withdrawal speed of 20 mm/min. However, comparing the samples it becomes clear, that higher preceramic polymer content also leads to thicker layers.

The surfaces of the samples with A and B ratios of the organic slurry seem to be smoother. The surface of sample 80B features a surface defect, where the coating has been removed, offering a view of the underlying substrate.

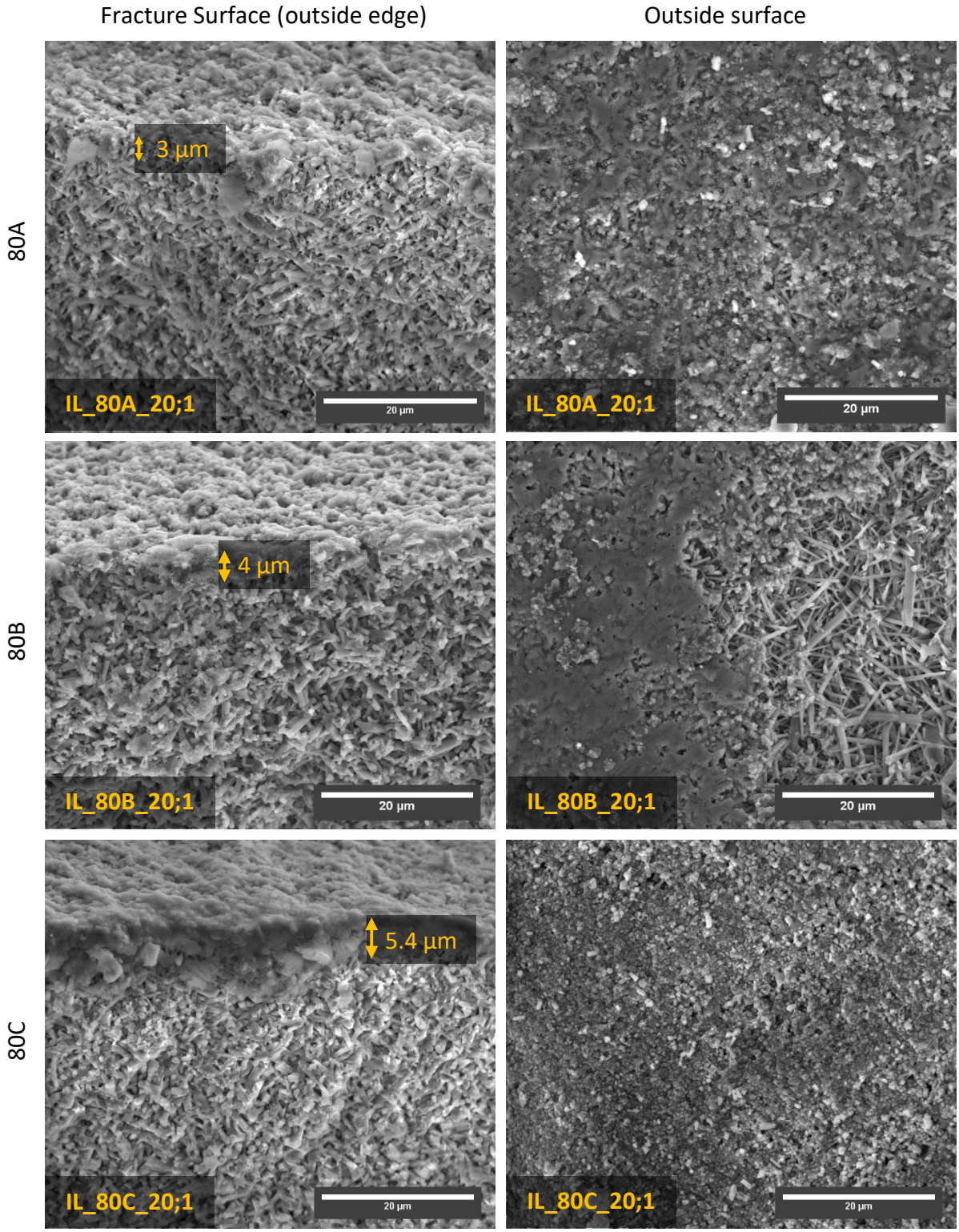

Figure 32: Micrographs of samples prepared with organic slurries of the same solvent content, but different ratios of silicon nitride to preceramic polymer

Variation of withdrawal speed

The samples were immersed for 1 second in an organic slurry with 80A composition. One was withdrawn with a speed of 20 mm/min and the other with 140 mm/min. Figure 33 shows the difference. The sample withdrawn with 20 mm/min has a much thinner layer on its surface, while the other sample has a very thick layer of 100 µm, which is not completely visible in the micrograph. The extremely thick layer might also be because of a defective masking, leading to a slip-casting like behavior and thus the thick layer.

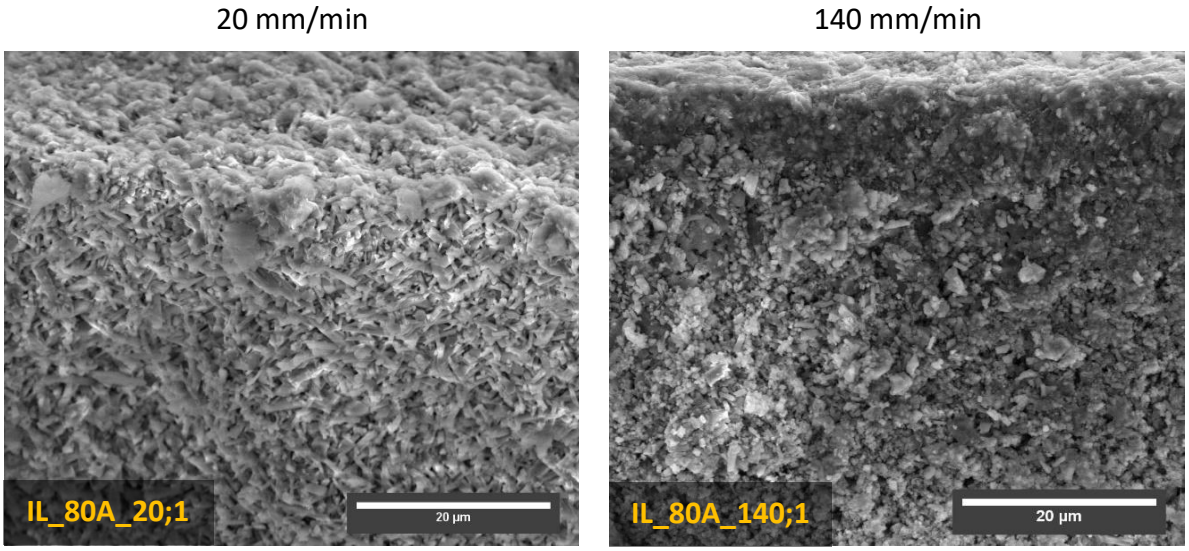

Figure 33: Comparison of fracture surfaces after pyrolysis of samples prepared with an 80A slurry at different withdrawal speeds

4.4.3 Problem of delamination

What was already visible in Figure 23 on a microscopic scale could also be observed in some samples on a macroscopic scale, shown in Figure 30. Delamination is a common occurrence, especially if the deposited layers are too thick. For the intermediate layer this behavior could basically always be observed, when the masking was not sufficient and slip casting with the organic slurries took place due to the unmasked pores pulling the liquid part of the organic slurry in.

4.5 Morphology of the separation layer

The following chapters show the morphology of the deposited separation layers.

Variation of masking solution

Figure 34 shows a comparison of samples masked by infiltration and then coated with the deposition fluid for the top layer with a withdrawal speed of 140 mm/min. The samples were pyrolyzed without removing the masking beforehand with toluene. Both samples show infiltration of the substrate and incomplete surface coverage of the layer.

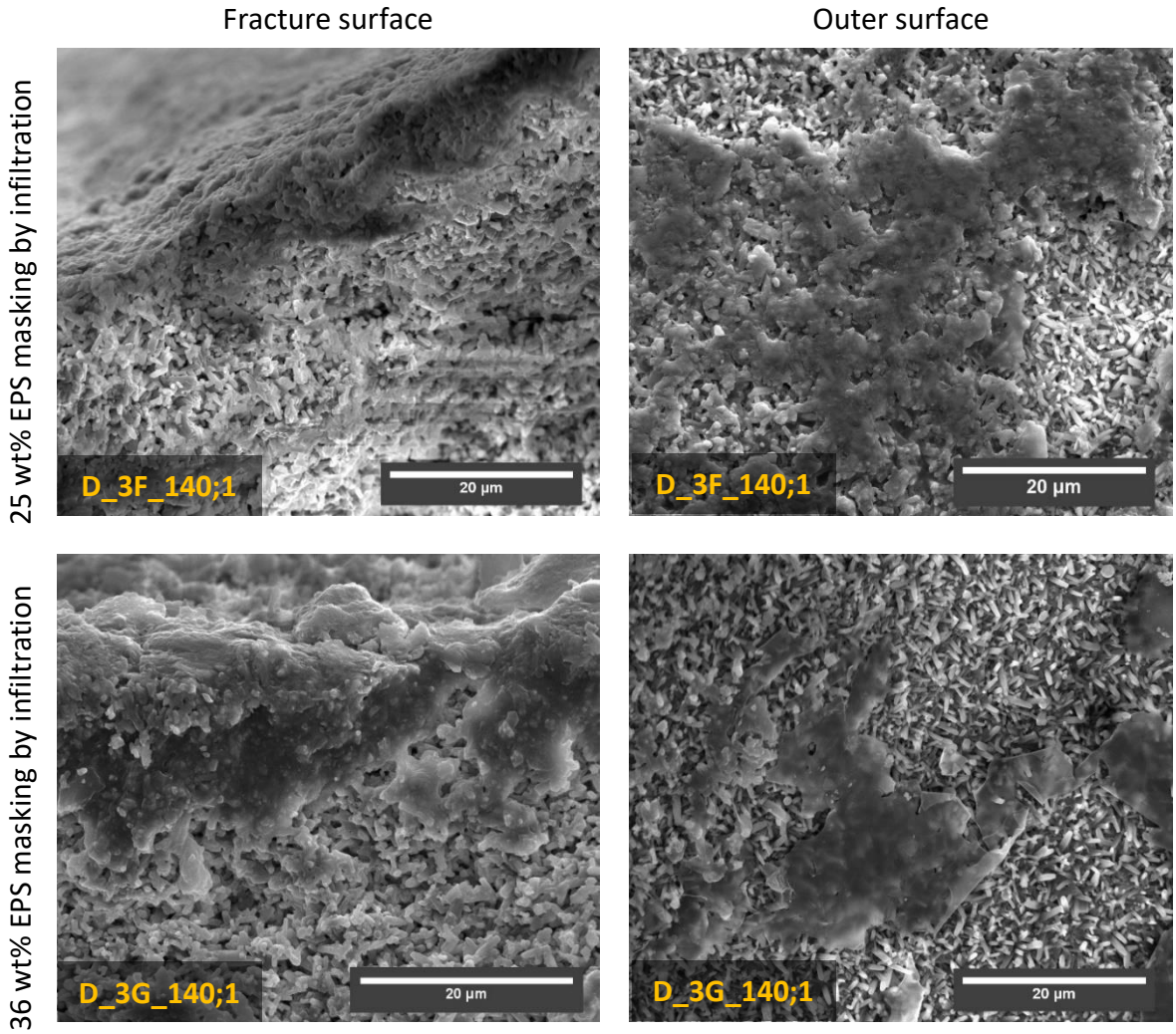

Figure 34: Comparison of samples that were masked by infiltration with differently concentrated masking solutions and then coated with a separation layer.

Variation of withdrawal speed for deposition step of separation layer

Figure 35 shows a comparison of the fracture surfaces of samples that were masked by immersion and then dip coated with the separation layer. The withdrawal speed from the deposition fluid was varied. The pyrolysis was carried out without removing the masking beforehand. This shows that the quality of the masking and handling of the samples in general is much more influential on the layer quality than the variation of coating parameters. What

was expected were slightly thinner layers for the samples prepared with 120 mm/min withdrawal speed. However, the sample morphology varies significantly, bare the fact that all samples show infiltration of the substrate, indicating a defective masking.

Figure 35a shows a thick outer layer that completely infiltrated the outer section of the substrate, leaving behind a seemingly dense layer. Figure 35b was prepared with only a slight change in withdrawal speed but it looks radically different. Even though infiltration had occurred, the deposition fluid did not completely fill out the pores of the substrate.

Figure 35c shows significant infiltration, probably due to a crack in the substrate, into which the deposition fluid could infiltrate better. Not considering the depth of infiltration the outer section of the layer looks very similar to what is shown in Figure 35a, which was prepared with the same withdrawal speed. In Figure 35d the macropores of the substrate are completely filled again, but it is very hard to find an actual layer thickness, since it is so irregular across the surface.

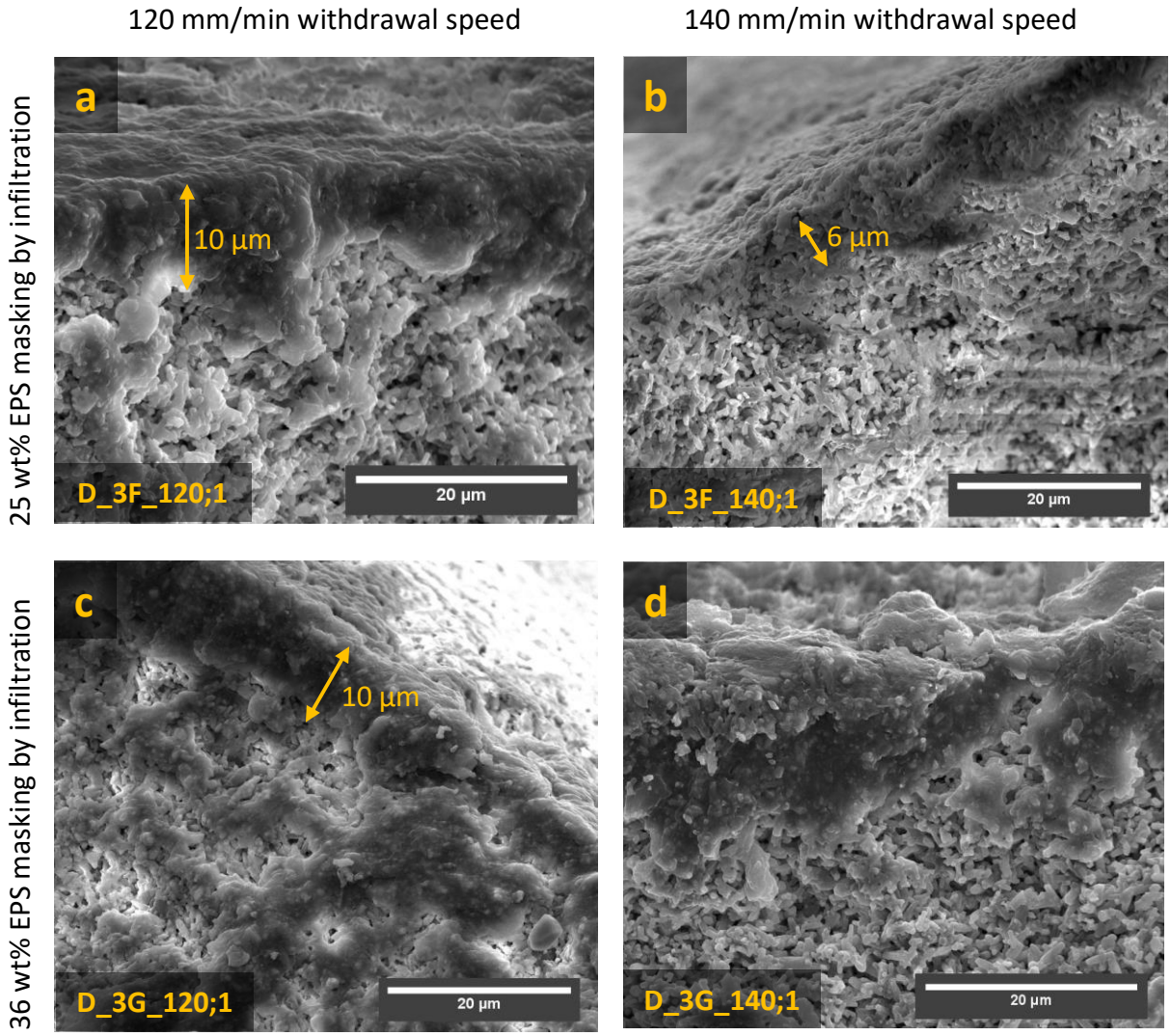

Figure 35: Variation of withdrawal speeds and masking for direct deposition of a separation layer onto masked substrates. The micrographs show fracture surfaces after pyrolysis.

Figure 36 shows another comparison of samples coated with different withdrawal speeds. Both samples were masked by dip coating with a 25 wt% EPS solution. The excess PS was removed by sanding before coating with the separation layer. The withdrawal speed in this coating step was varied for the samples. After crosslinking the masking was dissolved in toluene before pyrolysis of the layer.
It is not possible to compare the micrographs of the fracture surfaces, since one of them shows excessive infiltration, whereas the other shows a thin surface layer. The micrographs of the outer surfaces on the other hand suggest that the layer thickness of the sample prepared with lower withdrawal speed has a rougher surface and thus it can be concluded that the coating is thinner than on the other sample. Even though the sample prepared with higher withdrawal speed showed infiltration of the substrate, the outer surface is smooth with few surface defects.

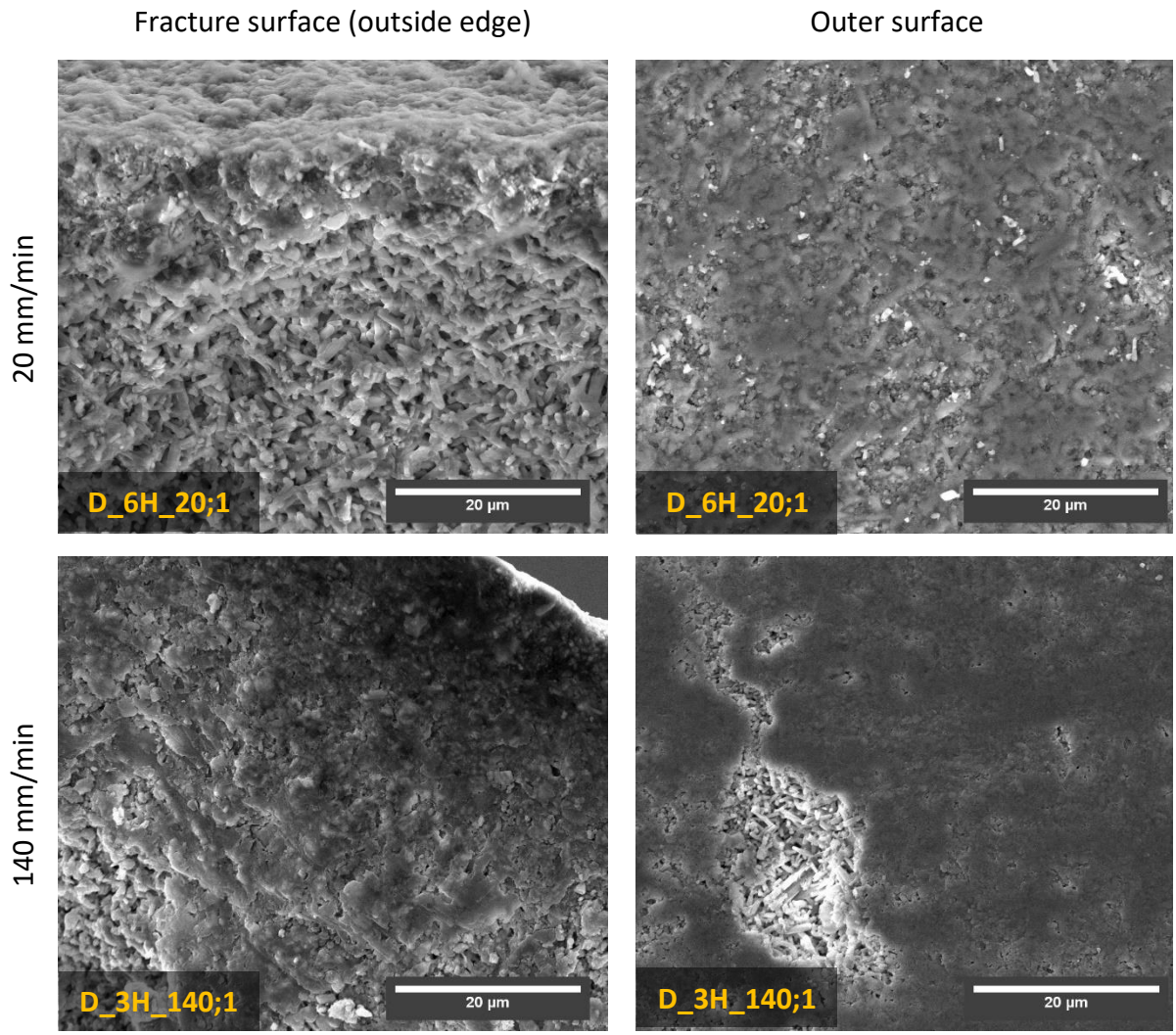

Figure 36: Variation of withdrawal speed from 20 mm/min to 140 mm/min

Direct coating on the inside of support tubes

Coating on the inside of the supports was thought to be an interesting alternative to the outside coating, since the inside of the tubes is much smoother due the nature of the slip casting process. The tubes were not masked for this process. Figure 37 shows a fracture surface and an inside surface of an unmasked sample that was dip coated with a separation layer on the inside with a withdrawal speed of 20 mm/min.

The fracture surface shows infiltration of the rod-like structure of the substrate, while the inside surface of the sample shows no dense layer.

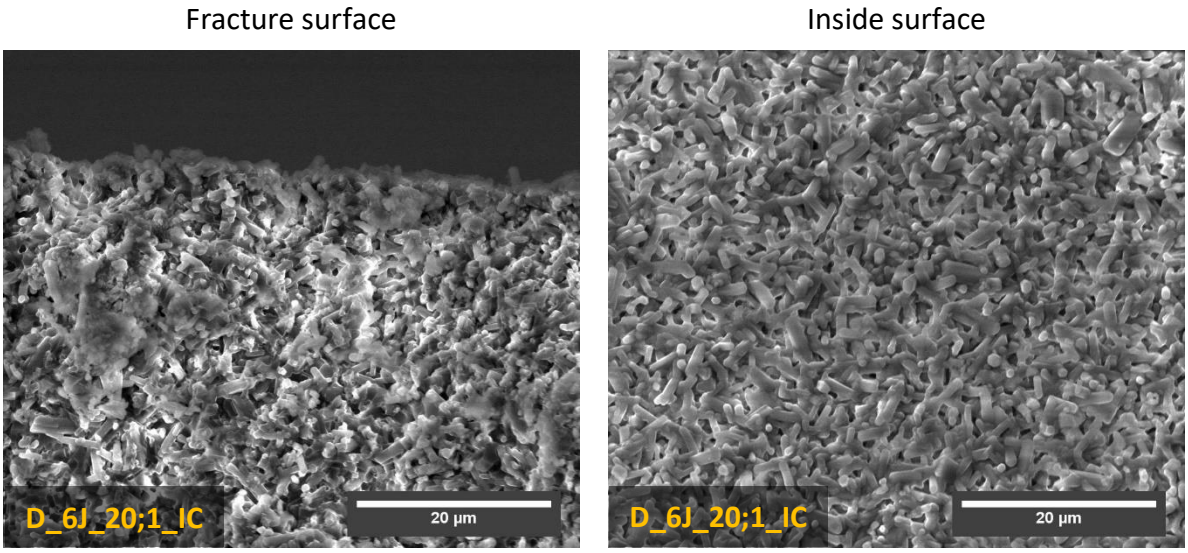

Figure 37: Directly coating separation layer on the inside of a substrate

Coating intermediate layer with separation layer

Most samples that were produced with an intermediate layer did not exhibit sufficient layer quality due to inhomogeneities or delamination, so micrographs could only be taken from one sample. An intermediate layer was applied onto this sample from an 80C organic slurry. It was then masked again, coated with the separation layer deposition fluid, crosslinked, the masking removed by toluene and then pyrolyzed. The fracture surface shows the intermediate layer with 12 µm thickness (compared to 9 µm that were shown in Figure 38). However, no separation layer can be observed. The outer surface does not show a separation layer either.

Fracture surface

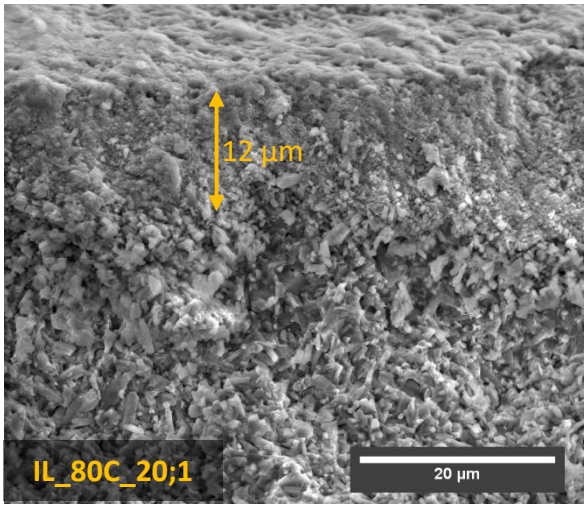

Outer surface

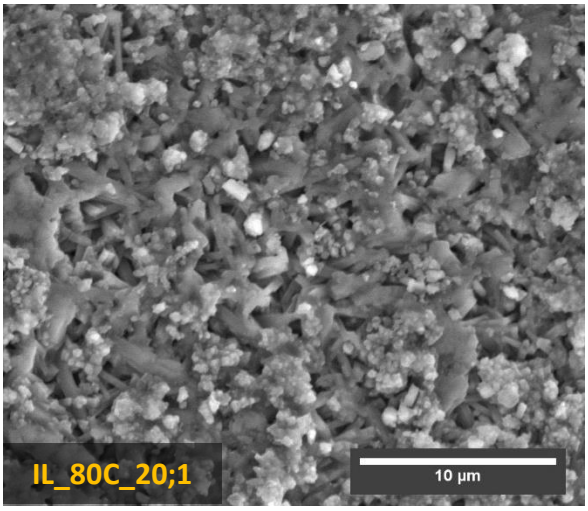

Figure 38: Intermediate layer coated with separation layer

5 Discussion

5.1 Tubular supports

The production of tubular supports has been thoroughly optimized by Thomas Prochaska, which is why there were no problems encountered during slip casting and sintering of the substrates.

Investigation of the aqueous Si_3N_4-slurries showed that they have high long-term stability, since rheological properties of a freshly prepared slurry and a slurry that had been prepared 70 days prior to the characterization showed no significant difference.

However, the comparison of properties of sintered samples prepared in prior works [41] and samples prepared over the course of this work does show a difference, which could be attributed to a malfunctioning pyrometer that had to be changed during this thesis. The old pyrometer would always overestimate the absolute temperature of the crucible in the hot press and thus regulate the heating power to lower values which were not consistent between runs. After changing the pyrometer, the maximum heating power at dwelling temperature was consistent. Since it is not clear whether or not the deviation of the old pyrometer was linear or not, nothing can be said about the way the heating and cooling phases were regulated. This leads to the conclusion that total heat transferred into the samples during the sintering process might not have been the same with the two different pyrometers.

Another indicator for this is that PTCR rings, which were used to get a better understanding of the hot press' heating profile, showed a significantly higher shrinkage, which can be correlated to a larger heat transfer, after installation of the new pyrometer.

Figure 39 shows the correlation of porosity and heating power at dwelling temperature of the respective sintering run. Blue data points show samples that were sintered using the old pyrometer, while green data points represent samples that were prepared using the new pyrometer. Red data points are from reference samples from a prior work [41].

The samples prepared with the new pyrometer were sintered with a higher heating power (and thus temperature) which lead to reduced porosity. When compared to the reference samples the same trend (higher heating power leads to reduced porosity) can be seen, however, there is an offset. Reference samples show a 1 % higher porosity.

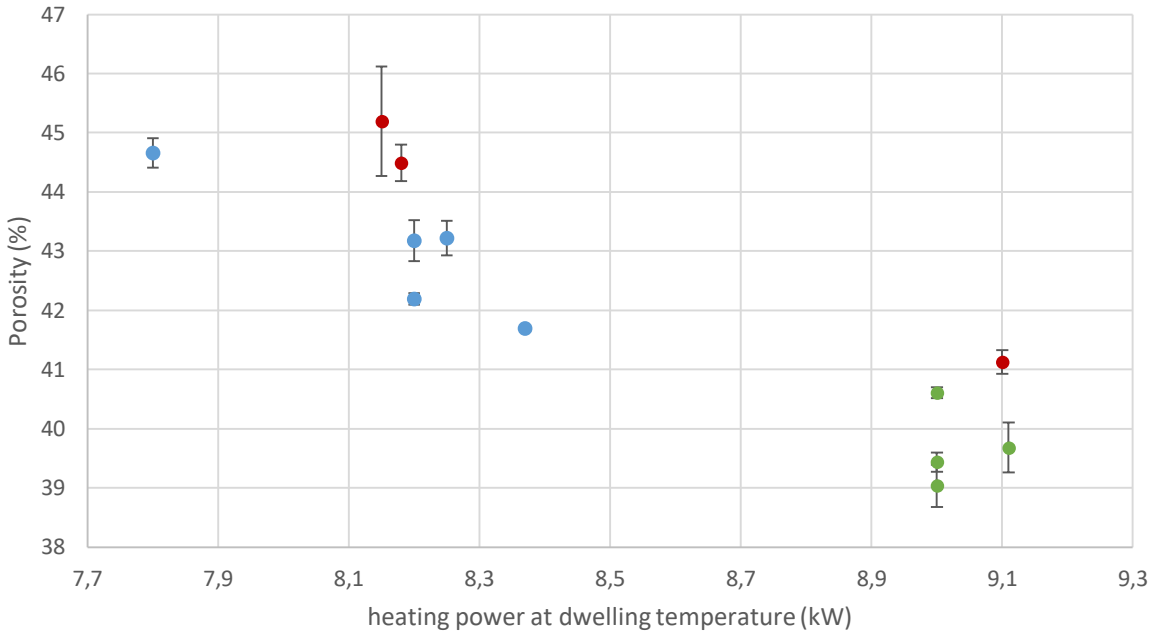

Figure 39: Correlation between heating power at dwelling temperature and porosity of samples prepared with the old (blue) and the new (green) pyrometer. Red data points were taken from [41]

Figure 40 shows the correlation of k_1 values against the heating power at the dwelling temperature of the sintering run for samples prepared with the old pyrometer (blue), the new pyrometer (green) and samples prepared in a prior work [41] (red). It shows that samples which were prepared with the old pyrometer match the samples of prior works much better than the samples sintered once the new pyrometer was installed.

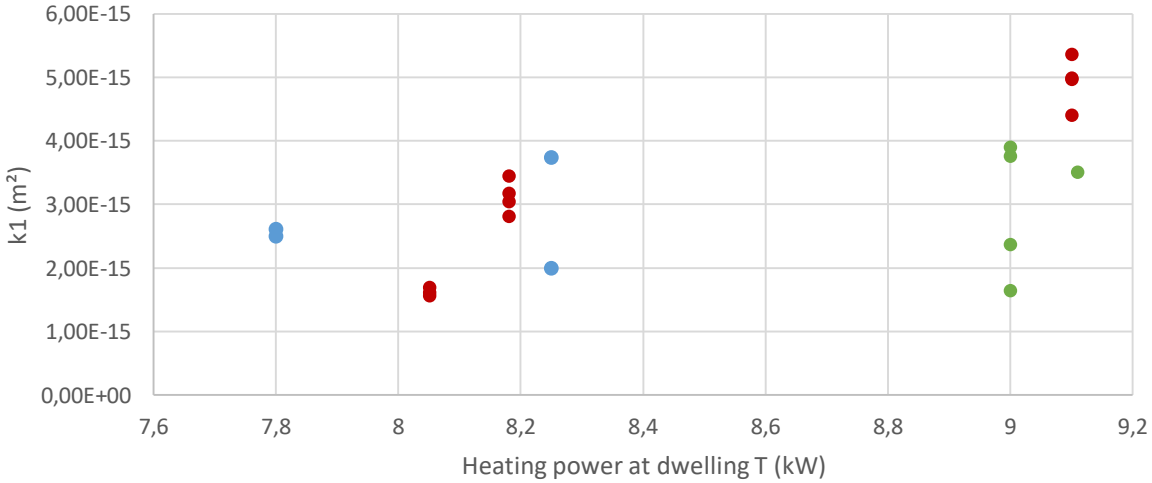

Figure 40: Correlation between heating power at dwelling temperature during sintering with the permeability (k1) of the samples. Blue data points represent samples prepared with the old pyrometer and green data points represent samples prepared with the new pyrometer. Red data points are taken from [41].

Figure 41 shows the correlation of sample porosity and k_1 values of the respective samples. Samples prepared using the old pyrometer are shown in blue, while samples prepared with the new pyrometer are shown in green. Red data points show reference values from a prior work [41]. This plot shows again, that samples prepared with the old pyrometer are much more consistent with the reference samples from a prior work, compared to the ones prepared using the new pyrometer. There is one outlier in the blue data points for which no explanation could be found. The reference samples show a higher permeability at the same porosity when compared to the samples prepared with the new pyrometer.

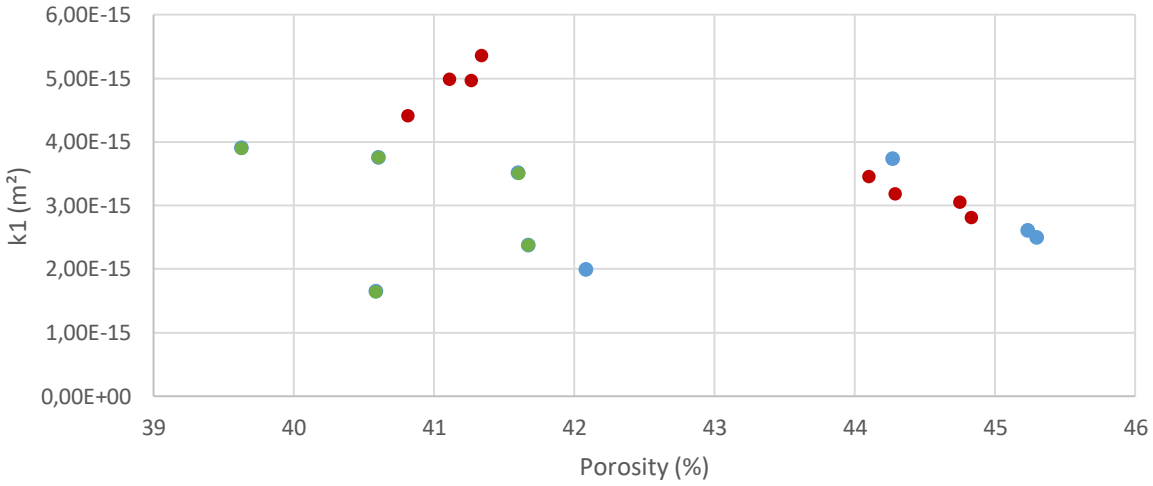

Figure 41: Correlation of Permeability (k1) and porosity of samples prepared with the old (blue) and the new (green) pyrometer. Red data points were taken from [41].

Despite the systematic offset in Figure 39 it can be concluded that the production process of the tubular supports is reproducible.

5.2 General observations for the dip coating process and SEM characterization

The produced layers were often times inconsistent. Most of those problems can be attributed to surface defects of the substrates or the masking process. This has to be considered when evaluating the results of the coatings on the samples.

Sample preparation for SEM only allows for small amounts of the samples to actually be observed. If the layers are very inconsistent across the surface, the micrographs might not be representative.

It also has to be considered that parameter variations for coating runs and the micrographs of the respective surfaces might lead to false conclusions, since it is almost impossible to accurately match for example layer thickness with deposition fluid concentration if the

dependency of the layer quality on an intact masking is much higher than any of the varied parameters.
In late stages of the work it was also observed that the deposition fluids sometimes did not wet the sample surfaces properly. This was only seen on substrates with very smooth surfaces (after sanding with P2000 SiC paper).
Delamination often occurs without being macroscopically visible. For example, the separation layer, is very thin and actually transparent, so delamination while handling or cutting the samples might not be spotted.

5.3 Masking of the tubular supports

5.3.1 Concentration of masking solution

Referring to Figure 19 it can be concluded, that the solutions containing 5 and 15 wt% EPS showed incomplete filling of the substrate pores, whereas the solutions with 25 and 36 wt% EPS both lead to comparable and usable results. Handling of the 25 wt% solution is much easier due to its lower viscosity.
The highly concentrated solutions led to the problem of leaving a rather thick PS layer on the sample surface, which had to be removed prior to subsequent coating steps. The removal is very delicate and most likely the reason why so many coatings failed over the course of this thesis. If PS is removed insufficiently, then the masking will be coated instead of the substrate. If too much material is removed, then the masked macropores might be abraded as well, leaving unmasked pores, which are infiltrated by the deposition fluids.
The latter is also a problem if the depth of infiltration of the masking is not consistent over the sample.
A solution to this problem was found by marking the surface of the substrate with a substance that does not dissolve in toluene or infiltrate the pores prior to masking.

5.3.2 Immersion vs dip-coating

Masking the samples by dip coating and immerson led to comparable results as shown in Figure 20. This makes masking by dip coating much more attractive compared to infiltration since less solution is lost in the process and it is less effort.

5.3.3 Type of polystyrene

According to the comparison in Figure 21 the type of polystyrene used has a big impact on the masking. In this work solutions made from EPS were primarily used. Tests showed that masking with a solution of 25 wt% commercially available PS with a molecular weight between 800 g/mol and 5000 g/mol in toluene led to insufficient filling of the pores, even though the solution was much simpler to handle because of its reduced viscosity and thus it left less excess PS on the outer surface of the substrate. It has to be investigated if a 35 wt% PS solution, which would most likely still be less viscous than the 25 wt% EPS solution, would suffice for masking. This could lead to a reduction of the thickness of the dense PS surface layer that has to be removed before coating. However, due to the low molecular weight of the

commercial PS this might not work at all. PS with longer chains can be bought from chemical suppliers as well, but suppliers usually guarantee a narrow distribution of chain length, which comes at a price, but is not important for our purpose at all. This is the reason why EPS, which has high chain lengths without a narrow distribution, wins out over commercially available PS for our intended purpose.

5.3.4 Substrate surface quality

For coating procedures, the surface quality has to be similar over the entire sample surface. At first it was assumed that this was the case for samples after sintering. The samples' roughness was also thought to aid in the layer adhesion according to [34]. During the investigation it was however found, that the roughness of the samples leads to inhomogeneous masking, and as a consequence to reduced intermediate and separation layer quality.

By polishing the sample surface before masking the masking quality could be improved significantly but it also reduced the apparent wetting of the samples. Often times there were patches of the sample that were not at all covered by the deposition fluid for the separation layer. This behavior could not be observed for the organic slurry, since the entirety of the sample surfaces were covered with the layer. Nevertheless, inhomogeneities due of the wetting behavior on polished samples have to be considered even during intermediate layer application.

Another point which has to be considered is that deep grooves - most likely stemming from the slip casting process or the handling of the green bodies - lead to surface defects in the layers. Excess masking solution leaves a layer that has to be removed before coating, however, if there is a deep groove filled with polystyrene, the coating solution for any of the following layers cannot get into contact with the substrate and consequently gets removed during dissolution or pyrolysis of the masking.

5.3.5 Alternative masking methods

The biggest issue with masking the samples is the excess PS left on the substrate surfaces. The removal of the right amount of PS on the outer surface is delicate and if a way to avoid it was found it would probably lead to a lower failure rate of the coatings.

Wrapping the samples with PTFE tape and then dipping them into a 25 wt% EPS- or PS-solution did not yield any usable results, since the solutions did not completely infiltrate the sample from the inside out.

An alternative masking method to avoid the dense PS surface coating may include applying the masking in multiple runs with less concentrated and thus less viscous solutions. This might also be possible in addition to covering the sample surface for example with PTFE tape before masking. The less viscous solution may penetrate the whole sample from the inside through to the surface.

5.3.6 Deposition liquid infiltration of the masked samples

Almost all micrographs show infiltration despite the masking. A theory is that although n-hexane might not dissolve polystyrene it might still have an effect on its structure and thus allow the infiltration. An indicator for such a behavior is the reaction of an EPS block that is dropped into n-hexane. It does not dissolve, but it shrinks.
It is also possible that the PS only coats the pore walls and leaves holes, which allow infiltration, behind.

5.4 Deposition and morphology of the intermediate layer

Organic slurry stability is of highest priority to produce homogenous intermediate layers. As can be seen in Figure 24, slurry stability decreases with higher solvent content, as well as higher preceramic polymer content.

5.4.1 Effect of stirring the organic slurry during dip coating

Although magnetically stirring the organic slurry during deposition worked well enough to counteract sedimentation for our tests, it does not yield reproducible results, which would be necessary for testing the performance of different separation layers, without having to take into account the influence of an inhomogeneous intermediate layer. The turbulence introduced into the system through stirring will never be consistent, since it depends on the geometry of the stirring bar and container used, the viscosity of the organic slurry and substrate geometry. By dipping the substrate into the slurry the turbulence is disturbed dependent on the fixation of the substrate, as well as dipping speed, holding time and withdrawal speed.

5.4.2 Poly(vinyl)silazane content

The preceramic polymer has a negative effect on slurry stability which is shown in Figure 24. A PSZ content leads to less slurry stability. From the micrographs it can be concluded that a higher poly(vinyl)silazane content in the organic slurry leads to increased intermediate layer thickness.

5.4.3 Influence of solvent on organic slurry

Stabilizing silicon nitride powder in n-hexane proved to be difficult. 2-butanone produced a stable organic slurry if the preceramic polymer content was kept low. However, 2-butanone reacts with poly(vinyl)silazane, and it dissolves polystyrene. A different solvent that produces stable organic slurries, like 2-butanone, but does not react with PSZ has to be found.
In order to find a better suited solvent, the restrictions for it need to be eased. Poly(vinyl)silazane reacts with any protic solvent as well as ketones and cannot be substituted. However, polystyrene, which is soluble in many different solvents may be substituted, with a polymer that does not dissolve as readily, since it is not actually a constituent of the final layer.

5.4.4 Effect of powder surface modification on slurry stability

Silicon nitride has a polar surface, covered with OH-groups if stored at a regular atmosphere. The modification of the powder surface through silanisation was evaluated but did not lead to improved results, as shown in Figure 26. However, only silanisation agents with relatively short organic tails were available for testing. Silanisation agents with longer organic groups like dodecyl- or octadecyltrimethoxysilane might be better suited for the task.
Other means of modification included the use of oleic acid, which was thought to reduce the powder particle interactions by adsorbing on the polar surface with its polar groups and reducing particle-particle interactions[49].
Even though it showed a positive effect on slurry stability for slurries with high preceramic polymer content it did not alter the behavior of the slurries with less polymer content.
Another approach for stabilizing organic silicon nitride slurries has been described by Iijima et al. [50]. They used a polyethyleneimine-oleic acid complex to stabilize the powder in toluene. It has to be investigated if this approach would also work for the n-hexane slurries used in our project.

5.4.5 Influence of solvent content on slurry stability

The samples that were prepared with an A-ratio of silicon nitride to polymer (3:1) show that the layer deposited from the fluid with the highest solvent content had the thickest layer in the micrograph (Figure 29), disregarding the obvious outlier. However, the same cannot be said for the samples prepared with B ratio (1:1) slips (Figure 31). They show much more similar layer thicknesses in the micrographs of the fracture surfaces. This might be because the withdrawal speed for the A-samples was much higher, which might amplify any effects that the different composition of the deposition fluid might have on the resulting layer thickness.

5.4.6 Influence of ratio of silicon nitride to poly(vinyl)silazane on slurry stability

The variation of silicon nitride content to preceramic polymer content in the slurries with constant solvent content showed in the micrographs of the fracture surfaces (Figure 32) that a higher content of poly(vinyl)silazane, which was supposed to act as a binder between the silicon nitride particles, leads to a denser layer (only looking at the fracture surface). The surface of the C-ratio (1:3) coated sample shows the least features of the underlying substrate which also means that the layer might be denser.

5.5 Coating of the intermediate layer

Since the intermediate layers produced often times were not homogenous or delaminated coating them could not really be investigated. From the few micrographs that were taken it can be said that multiple coating runs might be needed to be able to see an actual difference between the intermediate layer surface and the separation layer.

5.6 Direct coating of the separation layer onto masked substrates

The results of the different variations of the coating method that directly applies a separation layer to a masked substrate will be discussed below.

5.6.1 Effect of masking solution concentration

Judging from the micrographs of the fracture surfaces (Figure 34) one might conclude that the samples masked with 36 wt% EPS-solution show higher infiltration, however, the outer surface of the sample masked with the 36 wt% solution shows a very smooth layer, with features of the substrate visible, whereas the other sample seems thicker, with less substrate features visible.

It also has to be pointed out that the respective samples for this comparison were not treated with toluene before pyrolysis. This may lead to gas build up in the pores which might break the surface layer.

5.6.2 Effect of withdrawal speed

No significant difference could be seen in the micrograph (Figure 35) that compares samples that were prepared with 120 or 140 mm/min withdrawal speed. Masking quality as well as surface quality of the substrate have a much greater impact on the layer than this variation.

However, comparing the micrographs shown in Figure 36 it can be concluded that higher withdrawal speeds lead to thicker layers. The fracture surfaces do not allow for this conclusion because of the infiltration of one of the samples, but the micrograph of the outer surface of the sample that was withdrawn with 140 mm/min is much smoother and covers all features of the underlying substrate, whereas the sample prepared with 20 mm/min shows a surface through which the features of the substrate are still recognizable and would thus be much thinner.

This would also be in concordance with equation 1, in which the layer thickness is proportional to the withdrawal speed.

Micrographs of fracture surface with extremely deep infiltration may result due to a crack in the substrate through which the deposition fluid gets pulled in. The samples are more likely to fracture where an initial crack is already present, which explains why micrographs that show this infiltration behavior were very common for many of the samples.

5.6.3 Infiltration of the samples

Most of the coated samples showed infiltration of the substrate but a smooth surface with defects such as cracks (Figure 36).

It has to be investigated if the infiltration presents a problem, since the micrographs of the infiltrated samples look similar to what was expected from the intermediate layer. It is possible that the infiltrated macropores act as an addition bridging layer. During the infiltration and crosslinking the pores are completely filled, however, during the pyrolysis shrinkage occurs and gaps are likely to form.

The surface of such infiltrated samples is usually very smooth, which is also one of the requirements for the intermediate layer.
By finding a reproducible way to prepare infiltrated samples their porosity could be analyzed by mercury porosimetry to give insights into the pore formation.
Iwamoto et al. [22] have described something very similar to this proposition.

5.6.4 Surface defects

None of the samples that were directly coated were sanded before applying the masking, which might explain why surface defects like in Figure 36 were more often encountered.
Surface defects that remain on the sample might be covered by multiple applications runs for the separation layer.

6 Summary and conclusions

Partially sintered silicon nitride macroporous tubular supports were prepared by slip casting following a previously established process. Porosity as well as permeability measurements were conducted for the samples and the results compared to the previously prepared samples, which lead to the conclusion that even though there might be a systematic difference in porosity, the support preparation is reproducible.

However, one problem was found with the slip casting process: the surface quality of the substrates does not allow for deposition of defect-free layers. Through defects in the gypsum molds deep grooves or scratches are transferred onto the sample surfaces. A lack of green body stability in general allows for the introduction of even more defects onto the substrate surface. Such severe defects cannot be removed away properly.

An effective way of masking the substrates before application of coatings was found. EPS dissolved in toluene led to the best masking results after application by dip coating. The initially used immersion method was soon disregarded because dip coating led to comparable results while being less effort in general (using viscous solutions in the immersion apparatus (Figure 8) proved to be difficult). Furthermore, the solution is used much more efficiently. The best concentration for the masking solution was found to be 25 wt% EPS, since, according to the SEM micrographs, it completely filled the pores while being less viscous and thus easier to use than the 36 wt% solution. Solutions with lower concentrations than 25 wt% did not fill the pores completely.

It was also shown that using EPS as a cheap masking material works better than polystyrene that was bought from a chemical supplier. This is probably due to the average chain length of the polymers being greater for the EPS.

During the masking process a dense PS outer layer was created, which had to be removed prior to further coating steps. In initial trials either not enough of the PS was taken away, leading to the coating of the PS, which was then removed during pyrolysis, or too much was removed, resulting in the removal of the masked pores as well. To determine the exact amount of PS that had to be removed a metallic item, like a spatula or tweezers, were abraded on the silicon nitride surface of the substrate. This was done by abrasion of metallic items on the silicon nitride because using pens or sharpies lead to infiltration of the samples pores with ink/dye through capillary action.

As an alternative masking method the sample surface was wrapped with PTFE tape and then dipped into a 25 wt% EPS- or PS-solution. Neither approach yielded usable results.

Application of the intermediate layer was conducted via dip coating into an organic slurry composed of n-hexane, poly(vinyl)silazane and silicon nitride powder. The organic slurries were found not to be stable which is a prerequisite for a reproducible dip coating process.

To find ways to stabilize the slurries different compositions as well as oleic acid as an additive or modified powders were investigated. Even though slight stability improvements could be established for slurries with high poly(vinyl)silazane contents, no slurry was stable enough for a reproducible deposition method. Magnetically stirring the slurries during the dip coating step ensured that no sedimentation would take place but this is not a proper long term

solution for depositing reproducible layers, as it depends on too many processing variables, including stirring bar, container, and sample geometry or stirring speed.
The intermediate layer deposition also showed that insufficiently masked samples exhibit a slip-casting-like behavior when dipped into the organic slurry, leading to thick outside layers that delaminate easily, while also being infiltrated by the liquid components of the slurry, which results in pores of the substrate filled with preceramic polymer.
Coating the intermediate layers with a separation layer could not be investigated thoroughly due to a lack of usable samples.
Deposition of the separation layer directly onto the surface of the masked substrates by dip coating in a 1:1 n-hexane to poly(vinyl)silazane solution proved to be very promising. Disregarding surface defects, samples with very smooth and homogenous layers could be produced. By doing multiple coating runs the surface quality might be increased.
One problem that was encountered during the coating process was the infiltration of the masked samples with the liquid components of the deposition fluids. This is thought to be because of polystyrene's behavior in n-hexane. While it might not dissolve an EPS cube that is dropped into a beaker of n-hexane still exhibits shrinkage. Whether or not this is a problem has to be investigated, since the infiltrated macropores of the substrate might act as an intermediate layer by themselves, since the preceramic polymer fills the pores but then shrinks during pyrolysis, which suggests the assumption that cracks might form between the macropore walls and the polymer derived ceramic that they were filled with.

7 Outlook

Different masking materials should be investigated, since polystyrene proved to be restricting the whole coating process, as it narrows down the list of solvents that can be used for the preparation of the deposition liquids for the dip coating process.
For stabilizing the organic slurry in n-hexane, different additives have to be tested. Iijima et al. [50] managed to stabilize silicon nitride powder in toluene by using a polyethyleneimine and oleic acid complex. If another material is found to be usable as masking, then the solvent might be changed as well.
It has to be tested if the infiltrated macropores of the substrate can act as an intermediate layer. If that is the case, then deposition of an intermediate layer from an organic slurry might be skipped entirely.
Applying multiple separation layer coatings has to be tested. If surface defects can be counteracted this way, then a membrane could be realized.

8 Literature

[1] Jess, A. and P. Wasserscheid, *Industrial Hydrogen Production from Hydrocarbon Fuels and Biomass*, in *Hydrogen Science and Engineering : Materials, Processes, Systems and Technology*. 2016.

[2] Dong, J., Y.S. Lin, M. Kanezashi, and Z. Tang, *Microporous inorganic membranes for high temperature hydrogen purification.* Journal of Applied Physics, 2008. **104**(12): p. 121301.

[3] Wach, R.A., M. Sugimoto, and M. Yoshikawa, *Formation of Silicone Carbide Membrane by Radiation Curing of Polycarbosilane and Polyvinylsilane and its Gas Separation up to 250°C.* Journal of the American Ceramic Society, 2007. **90**(1): p. 275-278.

[4] Mori, H., S. Mase, N. Yoshimura, T. Hotta, K. Ayama, and J.I. Tsubaki, *Fabrication of supported Si_3N_4 membranes using the pyrolysis of liquid polysilazane precursor.* Journal of Membrane Science, 1998. **147**(1): p. 23-33.

[5] Salmang, H. and H. Scholze, *Keramik*. 7 ed. 2007, Berlin Heidelberg: Springer-Verlag.

[6] Shackelford, J.F., Y.-H. Han, S. Kim, and S.-H. Kwon, *CRC Materials Science and Engineering Handbook, Fourth Edition*. 2016, Boca Raton, UNITED KINGDOM: CRC Press.

[7] Eckel, A.J., *Silicon Nitride Rocket Thrusters Test Fired Successfully*. 2009.

[8] Herrmann, M., *Ceramic Bearings and Seals.* 2013: p. 301-328.

[9] Colombo, P., G. Mera, R. Riedel, and G.D. Sorarù, *Polymer-Derived Ceramics: 40 Years of Research and Innovation in Advanced Ceramics.* Journal of the American Ceramic Society, 2010. **93**(7): p. 1805-1837.

[10] Schmidt, H., D. Koch, G. Grathwohl, and P. Colombo, *Micro-/Macroporous Ceramics from Preceramic Precursors.* Journal of the American Ceramic Society, 2001. **84**(10): p. 2252-2255.

[11] Dismukes, J.P., J.W. Johnson, J.S. Bradley, and J.M. Millar, *Chemical Synthesis of Microporous Nonoxide Ceramics from Polysilazanes.* Chemistry of Materials, 1997. **9**(3): p. 699-706.

[12] Rouquerol, J., D. Avnir, C.W. Fairbridge, D.H. Everett, J.M. Haynes, N. Pernicone, J.D.F. Ramsay, K.S.W. Sing, and K.K. Unger, *Recommendations for the characterization of porous solids (Technical Report)*, in *Pure and Applied Chemistry*. 1994. p. 1739.

[13] Tsubaki, J., H. Mori, K. Ayama, T. Hotta, and M. Naito, *Characterized microstructure of porous Si_3N_4 compacts prepared using the pyrolysis of polysilazane.* Journal of Membrane Science, 1997. **129**(1): p. 1-8.

[14] Biesheuvel, P.M. and H. Verweij, *Design of ceramic membrane supports: permeability, tensile strength and stress.* Journal of Membrane Science, 1999. **156**(1): p. 141-152.

[15] Jüttke, Y., H. Richter, I. Voigt, R.M. Prasad, M.S. Bazarjani, A. Gurlo, and R. Riedel, *Polymer derived ceramic membranes for gas separation.* Chemical Engineering Transactions, 2013. **32**: p. 1891-1896.

[16] Prasad, R.M., Y. Iwamoto, R. Riedel, and A. Gurlo, *Multilayer Amorphous-Si-B-C-N/γ-Al2O3/α-Al2O3 Membranes for Hydrogen Purification.* Advanced Engineering Materials, 2010. **12**(6): p. 522-528.

[17] Kusakabe, K., Z. Yan Li, H. Maeda, and S. Morooka, *Preparation of supported composite membrane by pyrolysis of polycarbosilane for gas separation at high temperature.* Journal of Membrane Science, 1995. **103**(1): p. 175-180.

[18] Zhongyang, L., K. Kusakabe, and S. Morooka, *Preparation of thermostable amorphous Si·C·O membrane and its application to gas separation at elevated temperature.* Journal of Membrane Science, 1996. **118**(2): p. 159-168.

[19] Lee, L.L. and D.S. Tsai, *A Hydrogen-Permselective Silicon Oxycarbide Membrane Derived from Polydimethylsilane.* Journal of the American Ceramic Society, 1999. **82**(10): p. 2796-2800.

[20] Elyassi, B., W. Deng, M. Sahimi, and T.T. Tsotsis, *On the Use of Porous and Nonporous Fillers in the Fabrication of Silicon Carbide Membranes.* Industrial & Engineering Chemistry Research, 2013. **52**(30): p. 10269-10275.

[21] Miyajima, K., T. Eda, H. Ohta, Y. Ando, S. Nagaya, T. Ohba, and Y. Iwamoto, *Development of Si-N Based Hydrogen Separation Membrane.* Advances in Polymer Derived Ceramics and Composites, 2010.

[22] Iwamoto, Y., K. Sato, T. Kato, T. Inada, and Y. Kubo, *A hydrogen-permselective amorphous silica membrane derived from polysilazane.* Journal of the European Ceramic Society, 2005. **25**(2-3): p. 257-264.

[23] Ohji, T., *Porous Ceramic Materials*, in *Handbook of Advanced Ceramics: Materials, Applications, Processing, and Properties: Second Edition*. 2013. p. 1131-1148.

[24] Konegger, T., L.F. Williams, and R.K. Bordia, *Planar, polysilazane-derived porous ceramic supports for membrane and catalysis applications.* Journal of the American Ceramic Society, 2015. **98**(10): p. 3047-3053.

[25] Shibuya, M., T. Takahashi, and K. Koyama, *Microcellular ceramics by using silicone preceramic polymer and PMMA polymer sacrificial microbeads.* Composites Science and Technology, 2007. **67**(1): p. 119-124.

[26] Kalemtas, A., G. Topates, H. Özcoban, H. Mandal, F. Kara, and R. Janssen, *Mechanical characterization of highly porous β-Si3N4 ceramics fabricated via partial sintering & starch addition.* Journal of the European Ceramic Society, 2013. **33**(9): p. 1507-1515.

[27] Deville, S., *Freeze-Casting of Porous Ceramics: A Review of Current Achievements and Issues.* Advanced Engineering Materials, 2008. **10**(3): p. 155-169.

[28] Studart, A.R., U.T. Gonzenbach, E. Tervoort, and L.J. Gauckler, *Processing Routes to Macroporous Ceramics: A Review.* Journal of the American Ceramic Society, 2006. **89**(6): p. 1771-1789.

[29] Colombo, P., *Conventional and novel processing methods for cellular ceramics.* Philosophical Transactions of the Royal Society A: Mathematical, Physical and Engineering Sciences, 2006. **364**(1838): p. 109-124.

[30] Colombo, P. and J. Hellmann, *Ceramic foams from preceramic polymers.* Materials Research Innovations, 2002. **6**(5): p. 260-272.

[31] Binner, J.G.P., *Production and properties of low density engineering ceramic foams.* British Ceramic Transactions, 1997. **96**(6): p. 247-249.

[32] Scheffler, M. and P. Colombo, eds. *Cellular Ceramics*. 2005, Wiley-VCH Verlag: Weinheim.

[33] Landau, L. and B. Levich, *Dragging of a Liquid by a Moving Plate.* Acta Physicochimica U.R.S.S., 1942. **17**: p. 42-54.

[34] Grosso, D., C. Boissière, and M. Faustini, *Thin Film Deposition Techniques*, in *The Sol-Gel Handbook*. 2015, Wiley-VCH Verlag GmbH & Co. KGaA. p. 277-316.

[35] Busca, G., V. Lorenzelli, G. Porcile, M.I. Baraton, P. Quintard, and R. Marchand, *FT-IR Study of the surface properties of silicon nitride.* Materials Chemistry and Physics, 1986. **14**(1): p. 123-140.

[36] Vieth, S., M. Uhlmann, D. Linke, U. Klemm, D. Sobek, and F.-D. Börner, *Effect of surface silanisation on the dry pressing behaviour of silicon nitride powder.* Journal of the European Ceramic Society, 2003. **23**(1): p. 1997-2004.

[37] Yan, L.T., W.J. Si, S.W. Lin, H.Z. Miao, and L.H. Qi, *Influence of Coupling Agents on the Chemical Compatibility between Ultrafine Si3N4 Powders and Organic Binders.* Key Engineering Materials, 2002. **224-226**: p. 691-696.

[38] Grosso, D., *How to exploit the full potential of the dip-coating process to better control film formation.* Journal of Materials Chemistry, 2011. **21**: p. 17033-17038.

[39] Elyassi, B., M. Sahimi, and T.T. Tsotsis, *A novel sacrificial interlayer-based method for the preparation of silicon carbide membranes.* Journal of Membrane Science, 2008. **316**(1): p. 73-79.

[40] Hedlund, J., F. Jareman, A.-J. Bons, and M. Anthonis, *A masking technique for high quality MFI membranes.* Journal of Membrane Science, 2003. **222**(1–2): p. 163-179.

[41] Prochaska, T., *Porous Si3N4-based Support Materials with tailored Gas Permeability*. 2017, Vienna University of Technology: Vienna.

[42] Standardization, D.G.I.f., *DIN EN 623-2 Advanced technical ceramics. Monolithic ceramics. General and textural properties. Part 2: Determination of density and porosity*. 1993.

[43] Standardization, D.G.I.f., *DIN EN ISO 4022 Permeable sintered metal materials - Determination of fluid permeability*. 2006, DIN German Institute for Standardization.

[44] Konegger, T., *Tubular open-porous polymer-derived ceramic structures with tailored permeability*. 2016.

[45] Innocentini, M.D.M. and V.C. Pandolfelli, *Permeability of Porous Ceramics Considering the Klinkenberg and Inertial Effects.* Journal of the American Ceramic Society, 2001. **84**(5): p. 941-944.

[46] Drechsel, C., *Polymer-derived ceramic layer structures with multi-scale porosity*. 2016, Vienna University of Technology: Vienna.

[47] Duan, Y., J. Zhang, X. Li, Y. Shi, J. Xie, and D. Jiang, *Optimization of the tape casting process for the development of high performance silicon nitride substrate.* International Journal of Applied Ceramic Technology, 2017. **14**(4): p. 712-718.

[48] Gelest, I., *Silane Coupling Agents*, G. Inc., Editor. 2014.

[49] Tseng, W.J. and K.-H. Teng, *The effect of surfactant adsorption on sedimentation behaviors of Al2O3–toluene suspensions.* Materials Science and Engineering: A, 2001. **318**(1): p. 102-110.

[50] Iijima, M., N. Okamura, and J. Tatami, *Polyethyleneimine–Oleic Acid Complex as a Polymeric Dispersant for Si3N4 and Si3N4-Based Multicomponent Nonaqueous Slurries.* Industrial & Engineering Chemistry Research, 2015. **54**(51): p. 12847-12854.